Master's thesis

NTNU
Norwegian University of Science and Technology
Faculty of Medicine and Health Sciences
Department of Clinical and Molecular Medicine

Zuzanna Nowak

Macrophages as a modulator of PLA2G7 and DHRS9 in obesity in a depot dependent manner: implications in energy metabolism and inflammation

Master's thesis in Molecular Medicine
Supervisor: Pablo Miguel Garcia-Roves and David Sánchez-Infantes
Co-supervisor: Marit Walbye Anthonsen
June 2022

NTNU
Norwegian University of Science and Technology

UNIVERSITAT DE BARCELONA

Zuzanna Nowak

Macrophages as a modulator of PLA2G7 and DHRS9 in obesity in a depot dependent manner: implications in energy metabolism and inflammation

Master's thesis in Molecular Medicine
Supervisor: Pablo Miguel Garcia-Roves and David Sánchez-Infantes
Co-supervisor: Marit Walbye Anthonsen
June 2022

Norwegian University of Science and Technology
Faculty of Medicine and Health Sciences
Department of Clinical and Molecular Medicine

NTNU
Norwegian University of
Science and Technology

Acknowledgments

This project was performed during the years 2021-2022 at the Department of Physiological Sciences at the Faculty of Medicine and Health Sciences at the University of Barcelona as a part of the Erasmus exchange program between the University of Barcelona and my home university – Norwegian University of Science and Technology (NTNU) in Trondheim.

I am extremely happy and grateful that after one year of delay this exchange could eventually be arranged. This project would have not been possible without my two great supervisors: Pablo Miguel Garcia-Roves and David Sánchez-Infantes. I would like to express my deepest thanks to Pablo for all the guidance, help, patience and for keeping up with my stressed and chaotic self. I really appreciate everything I have learned at your laboratory. To David I want to say thank you for all the motivation you have given me through this whole process, for all the ideas that kept making this thesis better, and for showing me how it is to be a scientist (apparently, not easy). I am also grateful to other professors and students at the department who were always there to help me and made me feel welcome. I have to express my special gratitude to Norma Dahdah who made the days and the laboratory more exciting and taught me so much. I also want to thank my supervisor from NTNU - Marit Walbye Anthonsen since this thesis would have not been the same without all your valuable feedback.

Finally, I would like to thank my dear family and friends for experiencing with me all my struggles and successes and supporting me no matter what.

Zuzanna Nowak

Oslo, June 2022

Abstract

Many research studies have demonstrated that macrophages residing adipose tissue play a key role in obesity-induced inflammation. Therefore, the interplay between metabolism and immune system (immunometabolism) has been thoroughly investigated during recent years. Moreover, it appears that mitochondrial metabolism has an influence on macrophage polarization, adding another factor worth investigating in the context of immunometabolism.

In this project we aimed to identify genes that might play a role in a crosstalk between adipose tissue macrophages (ATMs) and adipocytes in subcutaneous and visceral white adipose tissue (sWAT and vWAT). PLA2G7 (encodes lipoprotein-associated phospholipase A2) and DHRS9 (encodes dehydrogenase/reductase 9) were selected as target genes for this thesis based on the quantitative analysis of provided datasets (from human and mice) that included groups of lean and obese individuals. We present that PLA2G7 and DHRS9 expression is elevated in ATMs from sWAT compared to vWAT in the individuals with obesity. We also show that these target genes are induced in WAT from humans and mice with obesity compared to lean individuals. RAW 264.7 mouse macrophage-like cell line was chosen as an *in vitro* method to study expression of PLA2G7 and DHRS9 under various conditions. RAW 264.7 cells were treated with palmitate and stimulated with LPS or IL-4 to examine whether these stimuli influence expression of target genes. We demonstrate that the expression of PLA2G7 and DHRS9 is elevated in RAW 264.7 cell line after LPS stimulation, but not after palmitate treatment. We also show that DHRS9 expression is increased after IL-4 activation. In conclusion, we propose PLA2G7 and DHRS9 as novel targets with a potential role in immunometabolism in obesity and related diseases. Additionally, our goal was to investigate subsequent states of mitochondrial respiration in RAW 264.7 cells stimulated with palmitate, LPS or IL-4. We used high resolution respirometry to measure oxygen consumption and oxygen flux in the treated cells. Our results indicate that palmitate treatment increase residual oxygen consumption in this macrophage-like cell line, while LPS/IL-4 activation leads to reduction in mitochondrial respiratory capacity.

Sammendrag

Mange forskningsstudier har vist at makrofager i fettvev spiller en nøkkelrolle i fedme-indusert inflammasjon. Derfor har samspillet mellom metabolisme og immunsystem (immunometabolisme) blitt grundig undersøkt de siste årene. Dessuten ser det ut til at mitokondriell metabolisme har en innflytelse på polarisering av makrofager, og legger til en annen faktor som er verdt å undersøke i sammenheng med immunmetabolisme.

I dette prosjektet hadde vi som mål å identifisere gener som kan spille en rolle i en krysstale mellom fettvevsmakrofager og adipocytter i subkutant og visceralt hvitt fettvev. PLA2G7 (som koder for lipoproteinassosiert fosfolipase A2) og DHRS9 (som koder for dehydrogenase/reduktase 9) ble valgt som målgener for denne oppgaven basert på kvantitativ analyse av gitte datasett (fra mennesker og mus) som inkluderte grupper av magre og overvektige individer. Vi presenterer at ekspresjon av PLA2G7 og DHRS9 er forhøyet i makrofager i fettvev fra subkutant hvitt fettvev sammenlignet med visceralt hvitt fettvev hos individer med fedme. Vi viser også at disse målgenene induseres i hvitt fettvev fra mennesker og mus med fedme sammenlignet med magre individer. RAW 264.7 makrofaglignende cellelinje fra mus ble valgt som en *in vitro* metode for å studere ekspresjon av PLA2G7 og DHRS9 under forskjellige forhold. RAW 264.7 celler ble behandlet med palmitat og stimulert med LPS eller IL-4 for å undersøke om disse stimuli påvirker ekspresjon av målgenene. Vi demonstrerer at ekspresjon av PLA2G7 og DHRS9 er forhøyet i RAW 264.7 cellelinje etter LPS-stimulering, men ikke etter palmitatbehandling. Vi viser også at DHRS9-ekspresjon økes etter IL-4-aktivering. Avslutningsvis foreslår vi PLA2G7 og DHRS9 som nye målgenene med en potensiell rolle i immunmetabolisme i fedme og relaterte sykdommer. I tillegg målet vårt var å undersøke påfølgende tilstander av mitokondriell respirasjon i RAW 264.7 celler stimulert med palmitat, LPS eller IL-4. Vi brukte høyoppløselig respirometri for å måle oksygenforbruk og oksygenfluks i de behandlede cellene. Resultatene våre indikerer at palmitatbehandling øker gjenværende oksygenforbruk i denne makrofaglignende cellelinjen, mens LPS/IL-4-aktivering fører til reduksjon i mitokondriell respirasjonskapasitet.

Table of contents

Acknowledgments i
Abstract ii
Sammendrag iii
List of abbreviations vi
1 Introduction 7
1.1 Obesity and diabetes 7
1.2 Characteristics of adipose tissue 7
1.3 Inflammation in adipose tissue 9
1.4 Macrophage subsets 10
1.5 Macrophages in obesity 12
1.6 Role of lipids in inflammation and atherosclerosis 13
1.7 Links between mitochondria and obesity 14
1.8 Genes modulated in adipose tissue macrophages 14
1.8.1 PLA2G7 encodes lipoprotein-associated phospholipase A2 15
1.8.2 DHRS9 encodes dehydrogenase/reductase SDR family 9 15
1.9 Aim of the study 16
2 Methodology 17
2.1 Database analysis 17
2.1.1 Database from human cohorts 17
2.1.2 Database from animal model 18
2.2 Cell culture 19
2.2.1 Palmitate treatment 19
2.2.2 Activation of M1 and M2 macrophages (LPS/IL-4 treatment) 19
2.2.3 LPS/IL-4 stimulation combined with palmitate treatment 19
2.3 High-resolution respirometry 20
2.4 Quantitative PCR (qPCR) analysis 22
2.5 Short hairpin RNA- mediated knockdown 23
2.6 Extraction and culturing of bone marrow derived macrophages (BMDMs) 23
3 Results 24
3.1 Two genes identified as potential novel targets in immunometabolism 24
3.1.1 PLA2G7 and DHRS9 are upregulated in sWAT macrophages compared to those infiltrated in vWAT in patients with obesity 24
3.1.2 PLA2G7 and DHRS9 gene expression is induced by obesity in humans 25
3.1.3 PLA2G7 and DHRS9 gene expression is induced by high fat diet in mice, and reduced by lifestyle intervention 26

3.2 High resolution respirometry of RAW 264.7 cells 26
3.2.1 After 24h palmitate treatment RAW 264.7 cells show increased residual oxygen consumption 27
3.2.2 LPS/IL-4 treated RAW 264.7 cells show decreased electron transfer capacity 29
3.3 Palmitate treatment does not induce expression of PLA2G7 or DHRS9 in RAW 264.7 cells 30
3.4 Expression of PLA2G7 and DHRS9 in RAW 264.7 cells is induced after LPS/IL-4 treatment 31
3.4.1 PLA2G7 is induced after LPS/IL-4 treatment in RAW 264.7 cells 31
3.4.2 RAW 264.7 cells treated with LPS/IL-4 show increased expression of DHRS9 32
3.5 LPS/IL-4 stimulation combined with palmitate treatment induces DHRS9, but not PLA2G7. 33
3.6 Culturing of bone marrow derived monocytes from lean and obese mice as an approach to assess expression of selected target genes 34
4 Discussion 35
5 Conclusions 40
6 References 41
7 Supplementary materials 46

List of abbreviations

ARG1	Arginase 1
AT	Adipose tissue
ATM	Adipose tissue macrophages
BMDMs	Bone marrow derived monocytes
BMI	Body mass index
CCL2	C-C Motif Chemokine Ligand 2
cDNA	Complementary DNA
DHRS9	Dehydrogenase/reductase 9
ECM	Extracellular matrix
ET	Electron transfer
eWAT	Epididymal white adipose tissue
FAs	Fatty acids
FFAs	Free fatty acids
FCCP	Carbonyl cyanide-p-trifluoromethoxyphenylhydrazone
HFD	High fat diet
IFN-gamma	Interferon gamma
IL-10	Interleukin 10
IL-12	Iterleukin 12
IL-4	Interleukin 4
Lp-PLA2	Lipoprotein-associated phospholipase A2
LPS	Lipopolysaccharides
NOX	NADPH oxidase
ox-LDL	Oxidized low-density lipoprotein
OXPHOS	Oxidative phosphorylation
PA	Palmitic acid
PLA2G7	Platelet-activating factor acetylhydrolase A2
PPIA	Peptidyl-prolyl cis-trans isomerase A
ROX	Residual oxygen consumption
shRNA	Short hairpin RNA
shSCR RNA	Short hairpin scramble RNA
SVF	Stromal vascular fraction
sWAT	Subcutaneous white adipose tissue
T2D	Type 2 diabetes
TGF-beta	Transforming growth factor beta
TGs	Triglycerides
TNF	Tumor necrosis factor
vWAT	Visceral white adipose tissue
WAT	White adipose tissue

1 Introduction

1.1 Obesity and diabetes

Obesity is an excessive accumulation or abnormal distribution of body fat that affects health and over the last few decades it has become a worldwide pandemic (1). According to World Health Organization (WHO), overweight or obesity causes over 4 million deaths per year. As many as 39% of adults were overweight and 13% obese in 2016. The problem also considers children and adolescents, with 18% of them being overweight or obese the same year (2). Cardiovascular diseases, musculoskeletal disorders, some cancer types and type 2 diabetes (T2D) are among the most prevalent comorbidities associated with obesity (3). Excessive fat might result in insulin resistance which is one of the first characteristic features in T2D pathogenesis. (4, 5). Increased prevalence of T2D in youth has been associated with family history of this condition, and with obesity (6). The connection between diabetes and obesity is evident, and these diseases have become a burden on social health care. Only in 2019 T2D was a direct cause of 1,5 million deaths (7). If nothing changes, the estimates show that by the year 2030 even 20% of world's adult population will be obese (8). Moreover, individuals with diabetes and obesity often experience chronic inflammation state and immune system dysfunction. These are the factors that might have an impact on the outcomes of infections, including SARS-CoV-2 disease, making even a greater strain on public health care (9).

1.2 Characteristics of adipose tissue

Adipocytes originate from mesenchymal stem cells (MSCs), which are pluripotent adult stem cells present in several types of tissues, including bone marrow and adipose tissue (AT). When triggered by signalling factors present in their microenvironment, MSCs convert into preadipocytes which eventually differentiate into adipocytes (**Figure 1A**) (10, 11). Apart from adipocytes, AT comprises of stromal vascular fraction (SVF) which includes, among others, adipose-derived stem cells, endothelial precursor cells, endothelial cells, pre-adipocytes and immune cells (including macrophages) (12). Interestingly, adipocytes can not only differentiate but also undergo a process called de-differentiation (**Figure 1A**). This occurs for instance during normal pregnancy and lactation, healing process and cancer development (10).

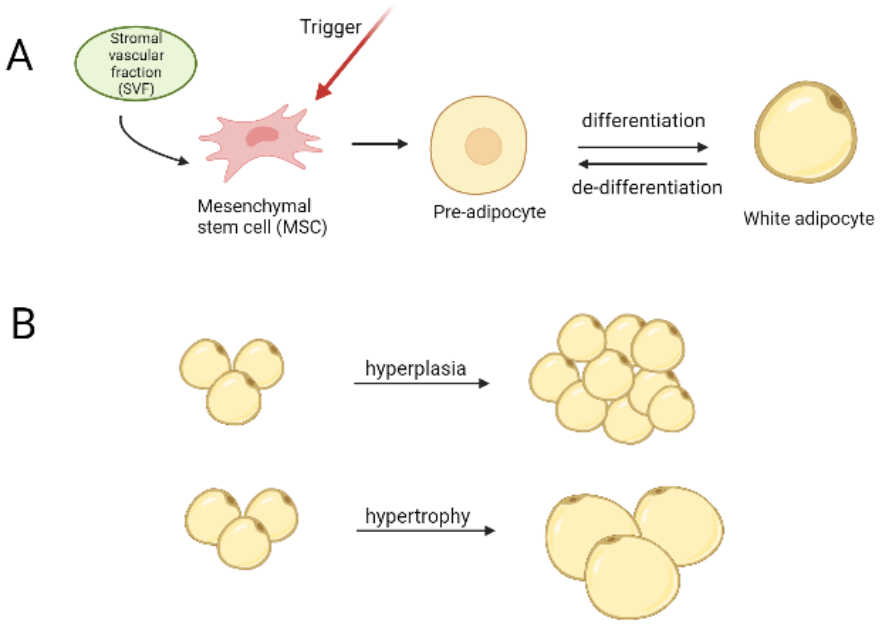

Figure 1: Adipose tissue biology. A: Adipocytes originate from mesenchymal stem cells (MSC) that are recruited from stromal vascular fraction (SVF). When triggered by signalling factors, MSCs differentiate into pre-adipocytes which later become adipocytes. If adipocytes undergo de-differentiation, they convert to a cell with a greater developmental potential. B: Two main mechanisms of coping with excessive fat in adipose tissue: hyperplasia is an increase in adipocyte number and hypertrophy is an increase of adipocyte size. Created with BioRender.com

There are two main types of AT: white AT (WAT) and brown AT (BAT). Adipocytes function as the body's fuel store, meaning that any surplus energy is deposited in WAT's adipocytes. BAT is characterized by its high number of mitochondria and its key role in heat production. Interestingly, upon cold stimulation WAT can undergo a process called 'browning' that results in beige/brown-like adipose tissue and its origin and function are under current investigation (13, 14). WAT is known for its plasticity and its percentage of body mass varies from around 20 to 28% in healthy individuals and goes as high as up to around 60% in cases of obesity (15). Key information on the factors that drive adipocyte plasticity is largely lacking. Among the known factors are some cytokines and properties of local microenvironment such as protein composition of extracellular matrix. Different ways of intracellular communication, such as microvesicles or a direct cell-to-cell contact also may have an impact, since plasticity-inducing signals may come from neighbouring cells (16). The properties of WAT define how the human body endure changes caused by obesity, but even the plasticity of AT is limited. If triglycerides cannot be stored in adipocytes, other organs,

like heart and liver, accumulate fat. However, the accumulation of ectopic fat in these organs may lead to toxic effects (17). Fortunately, before reaching that stage, excessive fat can be stored in one of several depots of AT. Subcutaneous WAT (sWAT) is a depot that accounts for most of the total amount of body fat. Due to that, primarily sWAT was linked to insulin resistance and other metabolic disorders. However, in subsequent research it was determined that expanded visceral WAT (vWAT, another depot of AT) is positively correlated with metabolic syndrome. The excess of vWAT increases a risk for coronary heart disease (without classical risk factors) and contributes to insulin resistance more than sWAT (13, 18, 19). There are two main mechanisms by which AT manages with excessive fat: via hypertrophy or hyperplasia **(Figure 1B)** (20). sWAT and vWAT show heterogeneity, and their characteristics change depending on the conditions they are exposed to. Studies on mice have revealed that sWAT and epididymal WAT (eWAT, depot of vWAT) have their unique characteristics and react to a high fat diet (HFD) exposure with a different adipogenesis rate. With hypertrophy being the first response to a calory excess in both sWAT and eWAT, it turned out that in prolonged HFD challenge the adipogenesis was initiated in eWAT. It was also showed that adipogenesis is not the main mechanism of sWAT to endure excessive fat accumulation (21, 22). Among already mentioned structural changes, WAT undergoes also remodelling of the vasculature and the extracellular matrix (ECM) (22). Besides being a fat storage, WAT is also a complex endocrine organ. AT secrets a wide range of adipocyte-derived proteins (adipocytokines), such as leptin, tumor necrosis factor alfa (TNF-alfa), interleukin-6 (IL-6) and monocyte chemoattractant protein 1(MCP-1). Several receptors are expressed in AT, such as insulin and glucagon receptors or TNF-alfa and IL-6 receptors (23, 24).

1.3 Inflammation in adipose tissue

Inflammation is an essential part of immune response, and it is induced to defend the host from infection that might be caused by various stimuli. In many cases acute inflammation is sufficient to resolve the damage caused by these stimuli. Interestingly, research showed that acute inflammation in adipose tissue is crucial by enabling proper remodelling and expansion of AT(25). The difficulty arises when the source of inflammation persists and/or anti-inflammatory responses are somehow impaired. Then the chronic inflammation occurs (26). It has been known for around 15 years that adipocytes generate immune response as a reaction to excessive fat (27), inducing chronic, low-grade inflammation termed meta-inflammation (28, 29). Although the primary trigger for meta-inflammation is not known, it is likely that hypertrophy and hyperplasia cause stressors like fibrosis and hypoxia (30). This chronic fibro-

inflammatory environment results in increased levels of cytokines and ECM proteins. Cytokines and ECM proteins may in turn impair adipogenesis and adipose tissue differentiation (22). Interestingly, in a research study conducted on diabetic and non-diabetic patients, fibrosis was determined to be a regulator of the balance between hyperplasia and hypertrophy (31). Considering all the findings during the past years, WAT is no longer only recognised as a fat storage and endocrine organ, but also as an immunological organ. When the fat expands, the adipose tissue begins to behave more as an immunological tissue and controls systemic inflammation and metabolism (32). TNF-alfa is one of the cytokines secreted by WAT and it was determined to be positively correlated with obesity and insulin resistance (33). As vWAT expands it begins to secrete more cytokines like IL-6 and TNF-alfa that further leads to recruitment of immune cells. When hypertrophy occurs in sWAT, levels of cytokines are comparatively lower (34). Research revealed that macrophages residing in AT are responsible for high expression of TNF-alfa and IL-6 (35), and that macrophage abundance increases with increasing body mass index (BMI) (36).

1.4 Macrophage subsets

Macrophages are derived from bone marrow hematopoietic stem cells that later differentiate into common myeloid progenitors and eventually into monocytes. Fully differentiated monocytes exit bone marrow and start circulating in the peripheral blood. From peripheral blood they can migrate into local inflammation sites, and this migration is mediated mainly by chemoattractants. After entering different tissues, monocytes differentiate into macrophages (37, 38). Macrophages' characteristics and names depend on the tissue they reside in. WAT attracts monocytes through monocyte chemoattractant protein-1 (MCP-1) and monocytes differentiate into adipose tissue macrophages (ATMs) at this site **(Figure 2)** (37).

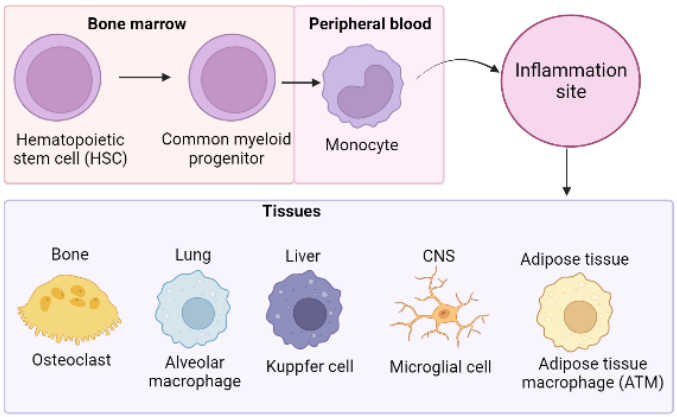

Figure 2: An illustration of macrophages' progenitors' migration and further differentiation. In the bone marrow hematopoietic stem cells (HSCs) differentiate into common myeloid progenitors. When common myeloid progenitors become monocytes, they exit bone marrow and start circulating in peripheral blood. From there they can easily reach various inflammation sites. Once monocytes enter a specific tissue, they differentiate into macrophages which are then tissue specific. CNS: central nerve system; Created with BioRender.com

Macrophages are primarily known as phagocytic cells, but they exhibit a great heterogeneity with respect to functions. For instance, they clear tissues by removing cells that have undergone apoptosis. While removing the cells that have died through necrosis, macrophages get stimulated to produce cytokines like TNF-alfa or IL-6. Moreover, the expression of their surface proteins changes (39). Two main polarizations of macrophages are usually distinguished: classically activated macrophages (M1), and alternatively activated macrophages (M2). M1 macrophages are induced by pro-inflammatory mediators such as TNF and interferon-gamma (IFN-gamma) and bacterial lipopolysaccharide (LPS) recognition. These cells contribute to immune response of T helper cells 1, mostly by phagocytosis and their microbicidal properties. M2 macrophages are driven by T helper cells 2 and play a role in anti-helminthic immune response, resolution and tissue repair phase, and have high endocytic clearance capacities (39, 40). However, the classification of macrophages is not straightforward and describing M1 macrophages as pro-inflammatory is accurate, while 'placing' M2 macrophages as their antagonists with 'anti-inflammatory' label is not quite right. M2 macrophages divide into following sub-groups: M2a, M2b and M2c. Each sub-group is activated by exposure to different molecules **(Figure 3)**. All the sub-types produce

high amounts of inflammatory cytokines, including M2b which is said to be the only one with anti-inflammatory properties. In general, M2 macrophages produce a lot of IL-10 and TGF-beta and show low levels of IL-12 (40, 41).

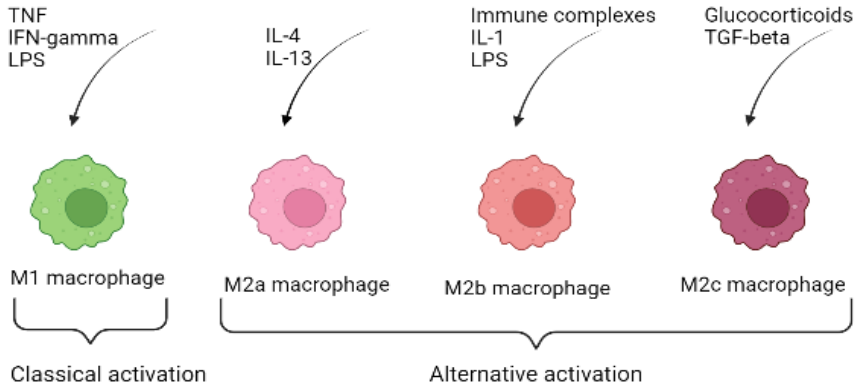

Figure 3: Different pathways of macrophage activation. Classical activation: M1 macrophages are induced through pro-inflammatory mediators such as TNF, IFN-gamma or LPS. Alternative activation: M2a macrophages are activates after exposure to IL-4 or IL-13, M2b activation is driven by immune complexes in combination with IL-1beta or LPS, and M2c macrophages are induced by TGF-beta or glucocorticoids. Created with BioRender.com

In recent years several pathways of macrophage polarization were identified. Among them we can find Signal Transducer and Activator of Transcription (STAT)-family, but also microRNAs and long non-coding RNAs (28).

1.5 Macrophages in obesity

As mentioned above, WAT is able to attract monocytes that later become ATMs and this attraction occurs in MCP-1-dependent manner. However, the process of macrophage recruitment is still under investigation and some studies suggest that free fatty acids (FFAs) released from AT can also work as recruiting signal for macrophages (37). Apart from the recruitment of macrophages, there remains a question of which type of macrophages that dominate in obese individuals' adipose tissue. Are macrophages able to switch their phenotype from more anti-inflammatory to pro-inflammatory? Or is it a M1/M2 – balance

that is being disturbed? Research shows that in lean mice the ATMs are polarized into M2 which produce high amounts of IL-10 that might help maintain normal adipocyte function and protect adipocytes against damaging effects of TNF-alfa and other cytokines. However, nutrient excess increases a new population of M1-polarized macrophages and with the M1/M2 balance being disturbed the protective effects of M2 ATMs are not longer sufficient. A decrease in quantity of M2 ATMs together with newly recruited M1 macrophages causes pro-inflammatory environment in AT with high amounts of TNF-alfa and IL-6 being secreted (42, 43). Other studies lean towards conclusion that ATMs adopt a different type of phenotype which is not entirely M1 or M2 (44). Furthermore, it was discovered that obesity-related factors can induce DNA hypermethylation at the peroxisome proliferator-activated receptor γ1 (PPARγ1) promoter, which was established to be a critical determinant of ATM pro-inflammatory activation (45).

1.6 Role of lipids in inflammation and atherosclerosis

Lipolysis is the hydrolysis of triglycerides (TGs) into glycerol and fatty acids (FAs). To be capable of crossing biological membranes, TGs need to be cleaved by lipases before moving in or out of cells. There are several processes where lipolysis is essential. One of them is the intracellular lipolysis that catalyzes the breakdown of TGs stored in intracellular lipid droplets so that fatty acids (FAs) can be released from WAT or used by the cells (in case of other tissues) (46, 47). FAs play an essential role as substrates in the synthesis of lipid membranes or lipids involved in cellular signalling. However, chronic excess of FAs might have harmful effects which in turn might cause mitochondrial disfunction, cell death or inflammation. These detrimental effects have been termed lipotoxicity (47, 48). Oxidized lipoproteins, FFAs and free cholesterol have pro-inflammatory and pro-apoptotic features that promote macrophage activation. Together with later modulation by lipid signalling these metabolites create a mechanism that underlies lipotoxicity in atherosclerosis or obesity-associated insulin resistance (49). As monocytes differentiate into macrophages during early stages of atherosclerosis, macrophage metabolism of oxidized low-density lipoprotein (ox-LDL) increases. In consequence, lipids are transported from the cells to the vessel walls. Development of atherosclerosis progresses when the levels of ox-LDL outrun the capacity of macrophage metabolism and the macrophages are transformed into foam cells (50).

1.7 Links between mitochondria and obesity

Potential changes in metabolic pathways such as Krebs cycle, oxidative phosphorylation (OXPHOS) and fatty acid oxidation might cause an impairment of immune cells. Importantly, these pathways play a role in macrophage polarization (51). Some of the intermediates provided by mitochondria have anti-microbial properties which help macrophages fight with pathogens. Other, like aspartate or itaconate provided by Krebs cycle, are critical for macrophage function (52). Interestingly, M1 and M2 macrophages use different metabolic pathways to provide energy supply. M1 macrophages depend more on high levels of glycolysis and pentose phosphate pathway. One should also keep in mind that all the involved metabolites can act as signals and therefore change M1 macrophages' function. M2 macrophages, on the other hand, use fatty acid oxidation and oxidative phosphorylation (OXPHOS). Each pathway is adjusted to each type's needs – glycolysis gives rapid energy supply at the inflammatory site, while OXPHOS provides energy for long-term processes (53). A study has shown that mitochondrial respiration is reduced in obesity and that mitochondrial oxidative capacity decreases with increasing BMI and systemic inflammation. However, it also revealed that ATP production was similar in lean and obese individuals which might be a compensatory mechanism to maintain energy production, or it might contribute to insulin resistance (36). Chronic inflammation is also associated with ATP consumption and ADP accumulation, as well as increased mitochondrial superoxide and oxidative damage, and all these events impede the resolution of inflammatory state (54). Interestingly, a study conducted on mice suggests that mitochondria can be intercellularly transferred from adipocytes to neighbouring macrophages. Mice on HFD had decreased mitochondria uptake by WAT macrophages and increased WAT mass, showing that this immunometabolic crosstalk is impaired in obesity (55). As a potential therapy, in another research study, an anti-inflammatory small-molecule drug was discovered to enhance ATMs oxidative phosphorylation and by that prevent or improve chronic inflammation and obesity-related disorders (56).

1.8 Genes modulated in adipose tissue macrophages

Throughout the years, many genes and signalling pathways have been associated with obesity (57). With time, studies started to focus on the connection between inflammation/immune cells and obesity. This journey continues to this day, revealing genes induced in AT in people with obesity that contribute to obesity complications. Most often these genes play a role in

inflammation and immune signalling (58). In this project we attempted to identify genes induced in ATMs and explore their role in immunometabolism. It resulted in choosing platelet-activating factor acetylohydrolase A2 (PLA2G7) and dehydrogenase/reductase 9 (DHRS9) as target genes for this thesis. Even though the selection of the genes is a part of the results, a brief background on PLA2G7 and DHRS9 is included to provide a better comprehension of the following parts of this thesis. More in-depth interpretation and explanation of the selection of PLA2G7 and DHRS9 as target genes is presented in the discussion (section 4).

1.8.1 PLA2G7 encodes lipoprotein-associated phospholipase A2

Over a decade ago lipoprotein-associated phospholipase A2 (Lp-PLA_2) emerged as an inflammatory marker that could be used to assess the risk for cardiovascular disease (59). Lp-PLA_2 is primarily produced by macrophages and PLA2G7 was identified as the gene coding for this enzyme. Moreover, it has been revealed that Lp-PLA_2 activity is strongly associated with genetic variants connected to LDL cholesterol levels (60, 61). Lp-PLA_2 cleaves oxidized phosphatidylcholine molecules that are produced during LDL oxidation. Through this cleavage, soluble pro-inflammatory and proapoptotic lipid mediators are being generated. These mediators are involved in recruitment and activation of leukocytes and macrophages that induce apoptosis and lead to defective phagocytic clearance which further enhance the progression of atherosclerotic plaques. It has been postulated that the inhibition of Lp-PLA_2 might help stabilizing atherosclerotic plaques (62). Interestingly, most of the plasma Lp-PLA_2 binds to low-density lipoprotein (LDL), while a smaller amount binds to high-density lipoprotein (HDL). The LDL-associated Lp-PLA_2 is reported to be a cardiovascular risk marker, while HDL-associated Lp-PLA_2 expresses antiatherogenic activities (63). Other beneficial activity of Lp-PLA_2 is decreasing of bioactivity of phospholipid substrates. Moreover, Lp-PLA_2 inactivates platelet-activating factor (PAF), which is involved in immune response and inflammatory diseases. It has been determined that PAF upregulates Lp-PLA_2 mRNA expression in monocytes/macrophages (64). The connection between Lp-PLA_2 and inflammatory responses in cardiovascular events might make it an interesting subject of investigation in the context of immunometabolism and obesity.

1.8.2 DHRS9 encodes dehydrogenase/reductase SDR family 9

DHRS9 gene codes for dehydrogenase/reductase SDR family member 9 which plays a role in androgen metabolic process and retinol metabolism (65, 66). Furthermore, DHRS9 was

identified as a stable biomarker of regulatory macrophages (an anti-inflammatory type of macrophages that is capable of suppressing T-cell proliferation) (67). Decreased expression of DHRS9 has been shown to correlate with progression of colorectal cancer (68), while its increased expression correlates with poor prognosis of pancreatic cancer (69). Connection between DHRS9 and immunometabolism is yet to be elucidated.

1.9 Aim of the study

Based on previous results obtained by our research group from transcriptomic analysis of macrophages infiltrated in sWAT and vWAT in patients with obesity, the hypothesis for this study is that depending on morphology and physiology of different WAT depots, ATMs behave differently in terms of gene expression. Therefore, a distinct crosstalk occurs between ATMs and adipocytes in sWAT and vWAT. Hence, the first step for this thesis was to analyse provided gene expression databases from sWAT and vWAT in humans and mice to select target genes. The main goal was to compare gene expression in WAT of lean and obese individuals in order to identify target genes that were significantly increased or decreased between these two groups. Ultimately this project aims to evaluate the specific role of the selected target genes in obesity and immunometabolism. Therefore, other aims for this project are as follows:

- Assess expression of chosen target genes in mouse macrophage-like RAW 264.7 cell line after palmitate, LPS and IL-4 treatment.
- Use high resolution respirometry to analyse subsequent states of mitochondrial respiration in RAW 264.7 cells treated with palmitate, LPS and IL-4.
- Silence one of the genes of interest in RAW 264.7 cells by the use of shRNA in order to investigate its expression after palmitate, LPS and IL-4 treatment in comparison to control groups.
- Examine expression of target genes *in vivo* by culturing of bone marrow derived monocytes collected from lean and obese mice.

2 Methodology

2.1 Database analysis

As mentioned above, database analysis was a crucial first step to identify target genes that might play a role in immunometabolism. Therefore, we focused particularly on finding genes that show significant difference in expression between control and obese group. Furthermore, we also studied the variation of gene expression between fat depots (sWAT and vWAT). To ensure the reliability of our results, we explored several databases that come from different models (human and mice cohorts). Statistical analysis of the data was performed in GraphPad (two-way ANOVA).

2.1.1 Database from human cohorts

Two separate databases were provided to perform quantitative data analysis and to compare gene expression between them. First cohort of human data was obtained from microarray analysis of macrophages isolated from sWAT and vWAT from obese patients (collected during bariatric surgery). In this group of patients 68% of them were female and 32% - male. Other patients' data are presented in **Table 1**.

Table 1: Clinical data of patients with obesity before bariatric surgery. The table shows mean values and ± SD. BMI: Body Mass Index.

Clinical parameters	**Values from patients with obesity**
Age	50.7 ± 9.9
Weight (kg)	112.1 ± 25.6
BMI (kg/m^2)	42.3 ± 6.7
Glucose (mg/dL)	103.2 ± 21.0
Total cholesterol (mg/dL)	191.1 ± 48.0
HbA1c (mmol/mol)	39.5 ± 6.0

To investigate whether the genes from the first dataset were modulated in obesity, rt q-PCR was performed in sWAT and vWAT from a second human cohort and included the following groups: control (lean individuals), metabolically healthy obese (MHO), metabolically unhealthy obese (MUHO). **Table 2** presents clinical data of the control group and obese patients (MHO and MUHO represented together).

Table 2: Clinical data of lean individuals and patients with obesity. The table shows mean values and ± SD. BMI: Body Mass Index.

Clinical parameters	Control group (n=14)	Patients with obesity (n=13)
Age	48.6 ± 8.22	46.2 ± 10.09
Weight (kg)	64.9 ± 9.40	112.2 ± 12.02
BMI (kg/m^2)	24.7 ± 2.55	43.5 ± 3.89
Glucose (mg/dL)	92.7 ± 15.43	106.5 ± 23.50
Total cholesterol (mg/dL)	190.0 ± 33.6	158.0 ± 18.0
HbA1c (mmol/mol)	31.5 ± 1.79	44.9 ± 11.17

2.1.2 Database from animal model

Second database was given by LiMa project which is a collaboration of several research groups. LiMa focuses on broadly defined metabolism and works often with animal models. The database provided by LiMa contained results from RNAseq of sWAT and eWAT from C57BL6/J mice. Mice were divided into three experimental groups: control, pathological (HFD), intervention (caloric restriction and exercise after HFD). Chosen phenotypical data of mice are adapted from (70), and presented in **Table 3**.

Table 3: Mice phenotype from three experimental groups: control, pathological (high-fat diet: HFD) and intervention group (caloric restriction and exercise after HFD). Presented data show mean values and ± SEM. White adipose tissue (WAT) values are normalized by body weight. Glucose values represent glucose concentration during intravenous glucose tolerance test.

Phenotype	Control group	HFD group	Intervention group
Body weight (g)	29.3 ± 0.24	43,2 ± 0.42	29,6 ± 0.21
WAT (g)	0.021 ± 0.001	0.046 ± 0.002	0.020 ± 0.002
Pancreas (g)	0.014 ± 0.001	0.026 ± 0.002	0.018 ± 0.001
TG in liver (ug TG/ug of protein)	193.0 ± 39.91	1582.1 ± 483.79	57.8 ± 18.47
Glucose (ng/mL)	69.6 ± 1.03	105.7 ± 3.40	119.8 ± 6.16

After the analysis of databases from human cohorts and animal model we were able to narrow down the list of genes of interest. Based on the results from statistical analysis we selected genes that have shown significant differences between the groups. To obtain information about the genes of interest and their possible relevance to immunometabolism, literature search was conducted using PubMed.

2.2 Cell culture

RAW 264.7 cell lines were kindly provided from prof. Ventura's laboratory (University of Barcelona). Cells were cultured in DMEM high glucose medium (Sartorius, #2145017) supplemented with 10% heat-inactivated Fetal Bovine Serum (FBS) (Biological Industries), 1% penicillin/strepromycin (Biological Industries) and 1% L-glutamine (Biological Industries), in humidified atmosphere of 5% CO_2 and at 37°C.

2.2.1 Palmitate treatment

40 mM of palmitic acid (PA) in a solvent of 0.1N NaOH/70% ethanol was prepared according to a protocol (71) and diluted in a full growth medium (DMEM, 10% heat-inactivated FBS, 1% penicillin/streptomycin, 1% L-glutamine) to obtain a final concentration of 0.1 mM and 0.3 mM PA. RAW 264.7 cells that reached 70-80% confluency were treated for 24 hours in either 0.1 mM PA, 0.3 mM PA, or without PA (controls). The cells were left for 24 hours in humidified atmosphere of 5% CO_2 at 37°C. After 24 hours of the treatment, the media was removed from and 500 µL of TRIsure™ (Meridian Bioscience, #120C) per well was added.

2.2.2 Activation of M1 and M2 macrophages (LPS/IL-4 treatment)

Starvation medium was prepared according to a protocol: DMEM (Sartorius, #2145017), 0.05% BSA (Sigma-Aldrich), 1% penicillin/streptomycin (Biological Industries). Following groups of RAW 264.7 cells were used in addition to regular RAW 264.7 cells for this treatment: RAW 264.7 cells with sh-RNA mediated knockdown of PLA2G7 (sh-PLA2G7), and RAW 264.7 cells containing scrambled shRNA (shSCR) (see section 2.5). All the groups of cells were left for 12h in starvation media in humidified atmosphere of 5% CO_2 at 37°C. Activation medium was prepared as follows: DMEM (Sartorius, #2145017) , 0.05% BSA (Sigma-Aldrich), 1% penicillin/streptomycin (Biological Industries) and activation molecule. Activation molecule for M1 macrophages was 60 ng/mL of LPS (Sigma-Aldrich), and for M2 macrophages – 40 ng/mL of IL-4 (Thermo Fisher Scientific). Cells were left for 12h in activation media in humidified atmosphere of 5% CO_2 at 37°C. After the treatment, the activation media was removed and 500 µL of TRIsure™ (Meridian Bioscience, #120C) per well was added.

2.2.3 LPS/IL-4 stimulation combined with palmitate treatment

RAW 264.7 cells were treated with combined treatment (PA with LPS/IL-4). Palmitic acid (PA) was prepared as described above (2.2.1) and a final concentration of 0.3 mM was obtained. 0.3 mM PA was mixed in DMEM (Sartorius, #2145017) with either LPS or IL-4

(Thermo Fisher Scientific) with the final concentration of 60 ng/mL and 40 ng/mL, respectively. Additionaly, there was one control group (non-treated cells) and one group only treated with 0.3 mM PA. The cells were left for 24 hours in humidified atmosphere of 5% CO_2 at 37°C.

2.3 High-resolution respirometry

Oroboros® delivers a technology that enables measurment of respiration at controlled oxygen levels, Oroboros® Oxygraph-2k was used to measure oxygen consumption in RAW 264.7 cell line after palmitate treatment (see section 2.2.1) and after LPS/IL-4 treatment (see section 2.2.2). Both experiments had a control group (RAW 264.7 cells without any treatment). DMEM was used as a calibration medium.

Four states of mitochondrial respiration were measured in intact cells. Before titration of any substrates, ROUTINE respiration was assessed. At this state respiration is controlled by cellular energy demand. After ROUTINE respiration, LEAK respiration was determined. LEAK respiration is the state when ATP synthase is not active (non-phosphorylating respiration) and it was measured after the titration of 2 µL of 4mg/ml (EtOH) oligomycin (ATP synthase inhibitor). Inhibition of ATP synthase was followed by titration of 3-5 µL of 4 mM carbonyl cyanide-p-trifluoromethoxyphenylhydrazone (FCCP). FCCP allows the maximal rate of O_2 consumption so that maximal respiratory capacity of the cells could be measured. This state of respiration is termed electron transfer (ET) capacity. Last of the measured states was residual oxygen consumption (ROX) which is the respiration due to oxidative side reactions. It was determined after the titration of 1 µL of 1mM (EtOH) rotenone and 1 µL of 5 mM (EtOH) antimycin A (AA). Rotenone and AA inhibit complex I and III, respectively. Each substrate (purchased from Sigma-Aldrich) was injected into each chamber after stabilizing of the slope signal. Graphic representation of the susequent states is presented below in **Figure 4**. The average oxygen flux rates were calculated for each state and corrected for background oxygen flux using the Datlab software (Oroboros Instruments). To normalize the data, protein assay of the cells was performed (data not shown). Statistical analysis was performed using GraphPad (t-test).

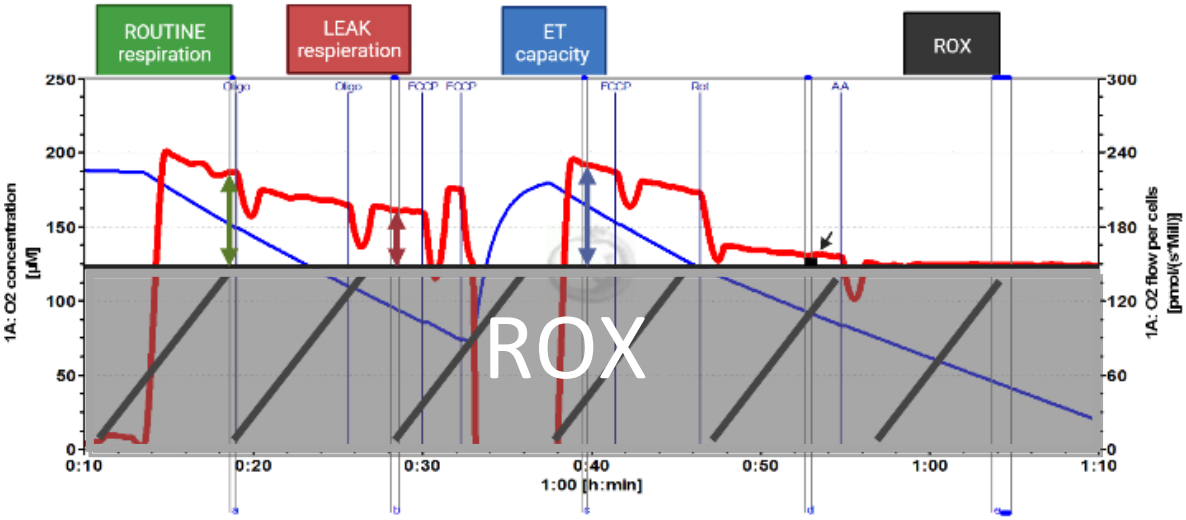

Figure 4: Subsequent states of mitochondrial respiration in RAW 264.7 cells and calculation of the respirator values. Blue line: O_2 concentration in the chamber (scale on the left). Red line: O_2 flow (respiration) (scale on the right). ROUTINE respiration: it is a physiological state in which respiration is controlled by cellular energy demand. Titration of oligomycin inhibits ATP synthase inducing not coupled (non-phosphorylating) LEAK respiration. LEAK respiration compensates for cation leak, pump slip and cation cycling, when ATP synthase is not active. Titration of FCCP (uncoupler) allows maximal rate of O_2 consumption, reflecting the electron transfer (ET) capacity in the non-coupled state. ROX is a term for residual oxygen consumption which is the respiration due to oxidative side reactions. ROX is induced after titration of rotenone (inhibitor of complex I) and antimycin A (inhibitor of complex III). Mitochondrial respiration is frequently corrected for residual oxygen consumption which is visualised in the figure with the darker background, black stripes and white ROX caption (72, 73). Therefore, the ROX values were subtracted from the raw values of ROUTINE respiration, LEAK respiration, ET capacity and ROX (after titration of rotenone and antimycin A). This is showed by green, red, blue and black arrows, respectively. Created with BioRender.com

2.4 Quantitative PCR (qPCR) analysis

Isolation of total RNA from the RAW 264.7 cells was performed by using Trisure™ (Meridian Bioscience, #120C), according to the manufacturer's instructions. Spectrophotometric analysis (NanoDrop One, Thermo Fisher Scientific) was carried out to assess the quantity and purity of the isolated RNA. cDNA was obtained through retrotranscription, with the use of synthesis kit (Thermo Fisher Scientific, #00690470). cDNA was used as a template for the qPCR reaction. In this project Taqman method was used to monitor the rt-PCR-process. In this method a hydrolysis of dual-labeled Taqman probes is followed by release of fluorophore. The release of fluophore generates fluorescence and the amount of fluorescence released during amplification is directly proportional to the amount of amplified DNA. qPCR was performed using a QuantStudio™ 7 Pro System (Applied Biosystems) in a 384 well-plate. Each well was loaded with 2 µL of cDNA of each sample and 9 µL of Mix. The Mix consisted of: 0.5 µL of TaqMan probe, 5.5 µL of SensiFAST Probe HI-ROX (Meridian Bioscience, #SFPH-920211A) and 3 µL of DEPC-water. During qPCR the cDNA was amplified in following states: holding state (2 min at 50°C and 10 min at 95°C) and cycling state (x40) with following steps: denaturation step (15 sec at 95°), annealing and extension steps (1 min at 60°) for a total duration of 1h 30 min.

A cDNA pool was obtained by mixing 8 µL of each sample into a tube and the standard curve for the gene expression studies was performed by the means of 1:4, 1:8, 1:16, 1:32, 1:64, 1:128, 1:256 dilutions. Gene expression was calculated as a fold change and normalized against the expression of PPIA. For some of the analysed genes standard curve could not be obtained and/or the samples had to be analysed without dilution. In these cases normalization against PPIA was not possible and the data were calculated as ΔCq. ΔCq values were obtained by subtracting of control group Cq mean values from the Cq values of all samples (including controls). This way, the higher abundance of a gene was detected (compared to control group), the lower ΔCq number was obstained. To make it clearer for the reader, the negative values were presented as positive (to show that the expression of a gene was higher), and consequently – positive values were shown as negative. Due to these calculations, mean values of controls were always approximately equal 0. Statistical analysis of the gene expression data was performed in GraphPad (t-test). The list over TaqMan assays ID can be found under Supplementary section, **Table S1**.

2.5 Short hairpin RNA- mediated knockdown

To carry out the knockdown of PLA2G7 gene in RAW 264.7 cells, a predesigned and validated short-hairpin RNA (shRNA) lentiviral vector was purchased from Sigma-Aldrich (Plko.1- PLA2G7-Puromycin glycerol stocks; Target Sequence: GCTTGTTACACAGTTGCCTTT; 3UTR). Plko.1-Scramble (Addgene) was used as control. GenEluteTM Plasmid Miniprep Kit (Sigma-Aldrich, #SLBV5605) was used to obtain pure plasmid DNA from the bacterial cultures. DNA concentration was measured using a Nanodrop spectrophotometer (Thermo-Scientific). Two independent PLA2G7 shRNA bacterial clones (1 and 2) were used to produce lentiviral infective particles in 293T cells. 293T cells were transfected using PEI MAX® (Polysciences) with the lentiviral vectors and the lentiviral vector packaging plasmids (PAX2 and VSV-G). After 3 days of incubation (37ºC and 5% CO_2), 293T cell supernatants containing the lentivirus vector were collected and filtered (0.22 µM). RAW 264.7 cells in 26th passage seeded in 6-well plates (60% confluence) were transduced with supernatants from clone 1, clone 2, Plko.1-SCR. WT RAW 264.7 controls were treated with mock medium from 293T cells. Polybrene® (Sigma-Aldrich) (4 µg/mL) was used to increase transduction efficiency. (Culturing conditions – see 2.2 cell culture). Cells were passaged from 6-well plate to 10cm dishes giving following RAW 264.7 groups: clone 1 (shPLA2G7-a), clone 2 (shPLA2G7-b), scrambled shRNA (shSCR), and WT control. Transduced cells were selected using 2 µg/mL of Puromycin (InvivoGen, #QLL-42-06) for 5-7 days. Only one clone was chosen for further experiments (LPS/IL-4 treatment). shPLA2G7 knockdown was validated by qPCR using shSCR as control.

2.6 Extraction and culturing of bone marrow derived macrophages (BMDMs)

Pairs of hind legs from 44 weeks old C57BL6/J mice were obtained. Mice were divided into following groups: High fat diet (HFD; diet-induced pathological group), Control (fed Standard Chow diet), Intervention-HFD (caloric restriction and exercise after HFD followed by another HFD) and Control-HFD (32 weeks on Standard Chow diet, 12 weeks on HFD). In total four bones were collected from each mouse: two femurs and two tibias. Isolation of bone marrow and culturing of BMDMs was carried out according to a protocol, with modifications (74).

3 Results

3.1 Two genes identified as potential novel targets in immunometabolism

It has been established that dysfunctional fat mass is tightly linked to our immune response. Therefore, a starting point for this project was analysis of the results from macrophage microarray data obtained from sWAT and vWAT of obese individuals. This was followed by quantitative analysis of two other sets of samples (from human and mice). Ranking and comparison of all the data resulted in selection of target genes that were significantly induced by obesity and differently expressed in vWAT compared to sWAT macrophages. These two genes are: Phospholipase A2 Group VII (PLA2G7) gene and Dehydrogenase/Reductase 9 (DHRS9) gene. The results from data analysis of PLA2G7 and DHRS9 expression are presented below.

3.1.1 PLA2G7 and DHRS9 are upregulated in sWAT macrophages compared to those infiltrated in vWAT in patients with obesity

Provided database from microarray of macrophages included transcriptomic analysis from sWAT and vWAT from 18 patients with obesity and different glucose levels (9 patients with glucose <100 mg/dl (healthy), and 9 patients with glucose >100 mg/dl (unhealthy)). PLA2G7 and DHRS9 show higher levels of gene expression in sWAT macrophages compared to vWAT macrophages. However, this depot modulation is only statistically significant in healthy patients (**Figure 5**).

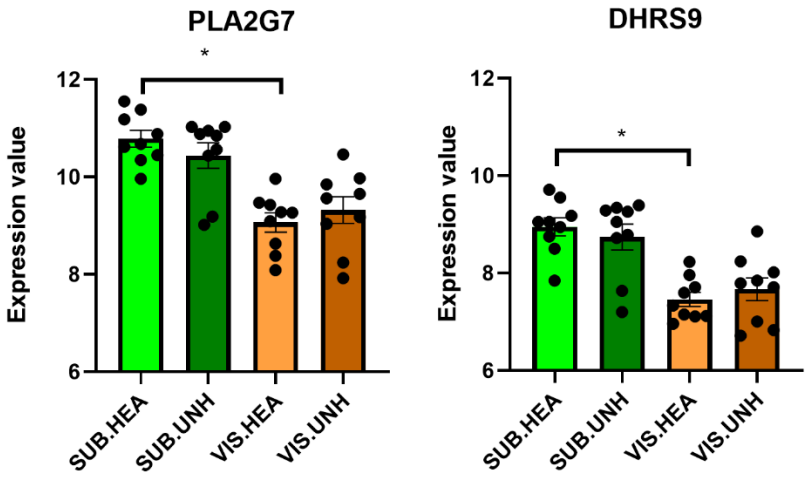

Figure 5: Levels of expression of PLA2G7 and DHRS9 gene in sWAT and vWAT in healthy and unhealthy obese individuals. Depot modulation is only statistically significant in healthy obese individuals (* $p < 0.05$). This figure represents mean and ± SEM values. The data were

obtained from microarray of macrophages collected from sWAT and vWAT of individuals with obesity. All statistical analyses of microarray data were performed in the R software environment. Quality control was performed using the arrayQualityMetrics package. Background correction, probeset summarization and normalization were performed with the oligo package using the most up to date annotation in Bioconductor. Initial evaluation through principal component analysis (PCA) detected outliers. A paired sample design comparing VAT and SAT from the same individuals was applied. SUB- subcutaneous adipose tissue, VIS- visceral adipose tissue, HEA- healthy obese, UNH- unhealthy obese.

3.1.2 PLA2G7 and DHRS9 gene expression is induced by obesity in humans

To study the role of our target genes in obesity, rt qPCR was performed in total sWAT and vWAT from an independent second human cohort. Samples were obtained from normal-weight individuals (controls) and individuals with obesity (metabolically healthy obese: MHO and unhealthy obese: MUHO). Our results show elevated expression levels of PLA2G7 and DHRS9 in obesity compared to control individuals. Moreover, higher levels were detected in sWAT compared to vWAT, observing the highest upregulation of these genes in sWAT from MUHO patients (**Figure 6**).

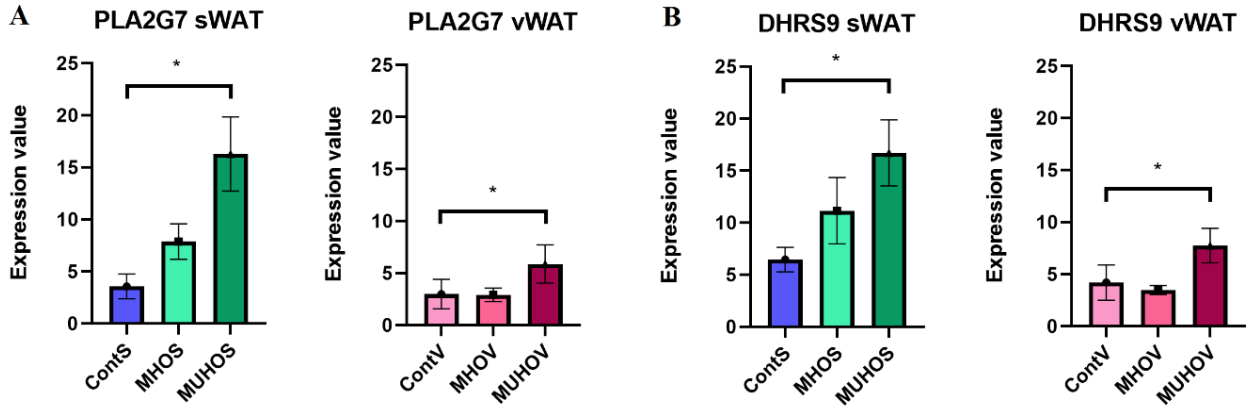

Figure 6: Expression of PLA2G7 (A) and DHRS9 (B) in sWAT and vWAT in a control group and in metabolically healthy and unhealthy individuals. The data represent mean values and ± SEM; * $p < 0.05$ ContS/ContV- control sWAT/vWAT, MHOS/MHOV- metabolically healthy obese sWAT/vWAT, MUHOS/MUHOV- metabolically unhealthy obese sWAT/vWAT.

3.1.3 PLA2G7 and DHRS9 gene expression is induced by high fat diet in mice, and reduced by lifestyle intervention

Dataset showed that PLA2G7 and DHRS9 appeared upregulated in eWAT from mice fed a HFD compared to lean mice and decreased after lifestyle intervention (**Figure 7**). The gene expression of both PLA2G7 and DHRS9 was very low in sWAT from mice and no modulation was observed with HFD or lifestyle intervention (**Figure S1**).

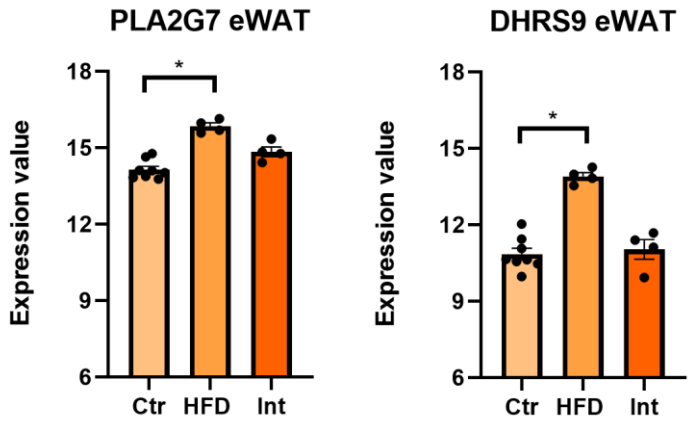

Figure 7: Levels of expression of PLA2G7 and DHRS9 in eWAT from mice. The data are divided into three groups: controls (Ctr, lean mice), high-fat diet fed (HFD, obese mice) and intervention (Int, mice on caloric restriction and exercise after HFD). The figure shows mean and ± SEM values; * p-value < 0.001.

Since our aim was to investigate the role(s) of our target genes (PLA2G7 and DHRS9) in immunometabolism, we have chosen mouse macrophage-like RAW 264.7 cell line as a model for our further experiments. In addition to having studied PLA2G7 and DHRS9 expression under various conditions (see section 3.3. and 3.4), we decided to test whether mitochondrial respiration of RAW 264.7 cells was altered after palmitate and LPS/IL-4 treatment. This way we could supplement this thesis with results that combine various macrophage stimulations with mitochondrial function.

3.2 High resolution respirometry of RAW 264.7 cells

In this project high resolution respirometry (Oroboros®, O2k Oxygraph) of RAW 264.7 cells was performed under various conditions: after palmitate (PA) treatment and after LPS/IL-4 activation. O_2 concentration and flux were measured after manual titration of following

substrates: oligomycin, FCCP, rotenone and antimycin A. This made it possible to determine respiratory capacities of RAW 264.7 cells in specific coupling states: ROUTINE respiration, LEAK respiration, electron transfer (ET) capacity and residual oxygen consumption (ROX). All the results shown later in this thesis are corrected for ROX and normalized by protein content.

3.2.1 After 24h palmitate treatment RAW 264.7 cells show increased residual oxygen consumption

Results from high-resolution respirometry of RAW 264.7 cells show that ROUTINE respiration, LEAK respiration and ET capacity are not significantly influenced by the different PA concentrations in RAW 264.7 cells (**Figure 8A,B,C**). Inhibition of complex I by rotenone showed a slight increase in oxygen consumption in the PA treated cells, but not significant (**Figure 8D**). After titration of antimycin A (inhibitor of complex III) residual oxygen consumption could be evaluated and a significant increase in the cells treated with 0,3 PA, comparing to non-treated control group was observed (**Figure 8E**). Reserve capacity (ET capacity subtracted by ROUTINE respiration) and ROUTINE respiration corrected by LEAK respiration (net OXPHOS capacity – ATP production) are not significantly changed after PA treatment, although the values for 0.3 PA group are slightly lower. (**Figure 8F,G**). Results presented below in Figure 8 are obtained from two independent experiments.

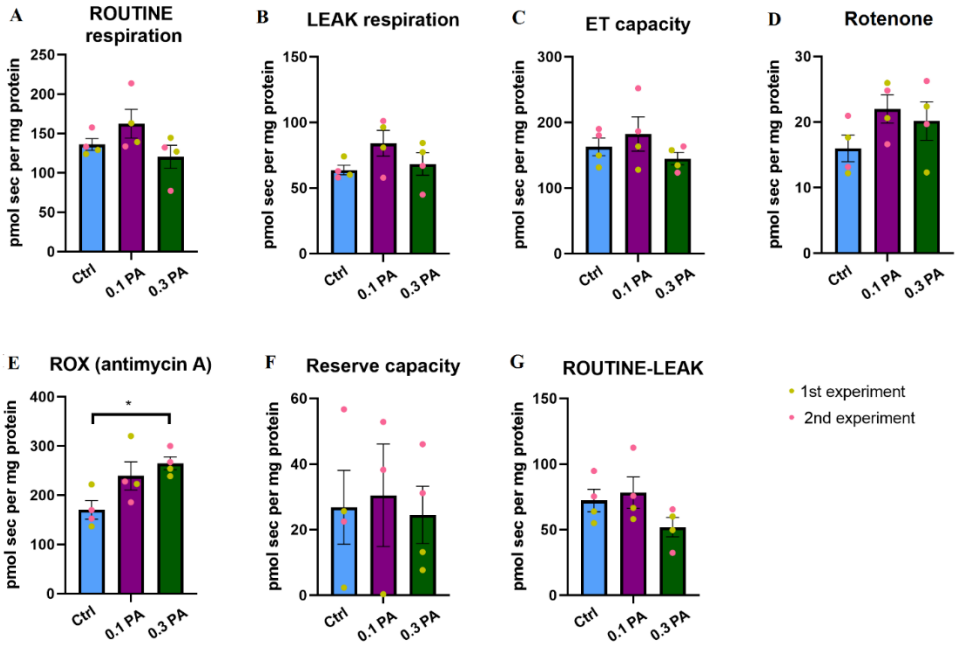

Figure 8: States of mitochondrial respiration in RAW 264.7 cells after palmitate treatment (0.1 mM PA and 0.3 mM PA), and in non-treated controls. ROUTINE respiration (A), LEAK

respiration (B) and ET capacity (C). Inhibition of complex I by rotenone (D) and complex III by antimycin represents residual oxygen consumption (ROX) (E). Reserve capacity is the ET capacity subtracted by ROUTINE respiration (F). ROUTINE respiration corrected by LEAK respiration (G) is the coupled respiration that shows net OXPHOS capacity – ATP production. Presented results come from two independent experiments (yellow-green and pink dots). Results are presented as mean values and ± SEM; * p-value < 0.05.

To express respiration independent of cell count, flux control ratios normalized for ET capacity were used as an internal normalization (**Figure 9**). To assess how close ROUTINE respiration is to ET capacity, R/E control ratio was calculated. The differences between control group and treated group are not significant (**Figure 9A**). Dyscoupled respiration under pathological conditions is related to mitochondrial dysfunction. To investigate uncoupling or dyscoupling at constant ET capacity, L/E coupling-control ratio was determined. Obtained results do not show any increase or decrease between the groups (**Figure 9B**). Values after rotenone titration normalized for ET capacity show no significant difference in the treated cells (**Figure 9C**). Similar as in Figure 8, ROX values after antimycin A titration are increased after 0.3 mM PA treatment also after normalization for ET capacity (**Figure 9D**).

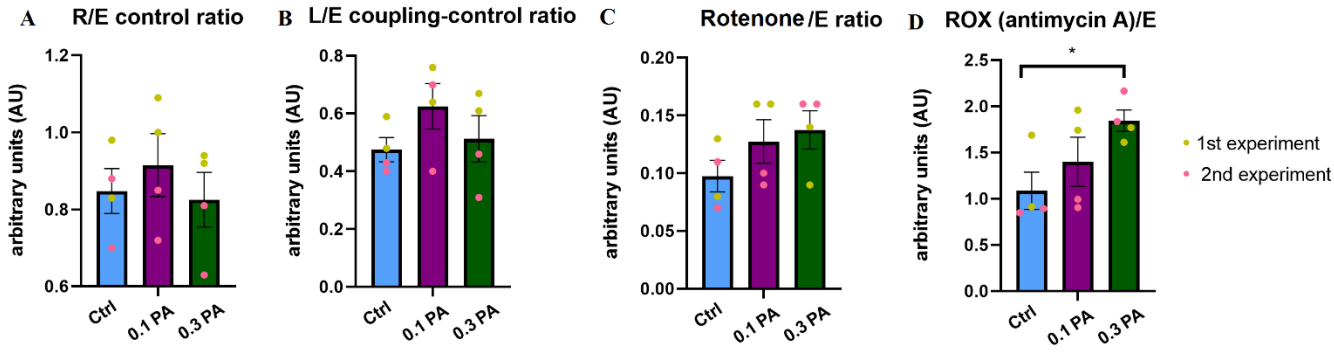

Figure 9: Data from high resolution respirometry of RAW 265.7 cells after PA treatment normalized for ET capacity. R/E control ratio expresses how close ROUTINE respiration operates to ET capacity (A). L/E coupling-control ratio is an index of uncoupling or dyscoupling at constant ET capacity (B). Figure represents also oxygen fluxes after rotenone and antimycin A titration normalized for ET capacity (C and D). Presented results come from two independent experiments (yellow-green and pink dots) Results are presented as mean values and ± SEM; * p-value <0.05.

3.2.2 LPS/IL-4 treated RAW 264.7 cells show decreased electron transfer capacity

ROUTINE respiration and LEAK respiration in RAW 264.7 cells are not significantly influenced by the LPS/IL-4 stimulation (**Figure 10A,B**). Electron transfer (ET) capacity significantly falls after LPS/IL-4 treatment comparing to non-treated control group (**Figure 10C**). Reserve capacity also declines after the treatment (**Figure 10F**). Net OXPHOS capacity presented as ROUTINE corrected by LEAK respiration and ROX consumption are not significantly altered after the treatment (**Figure 10D,E,G**). Results presented below in Figure 10 are obtained from two independent experiments.

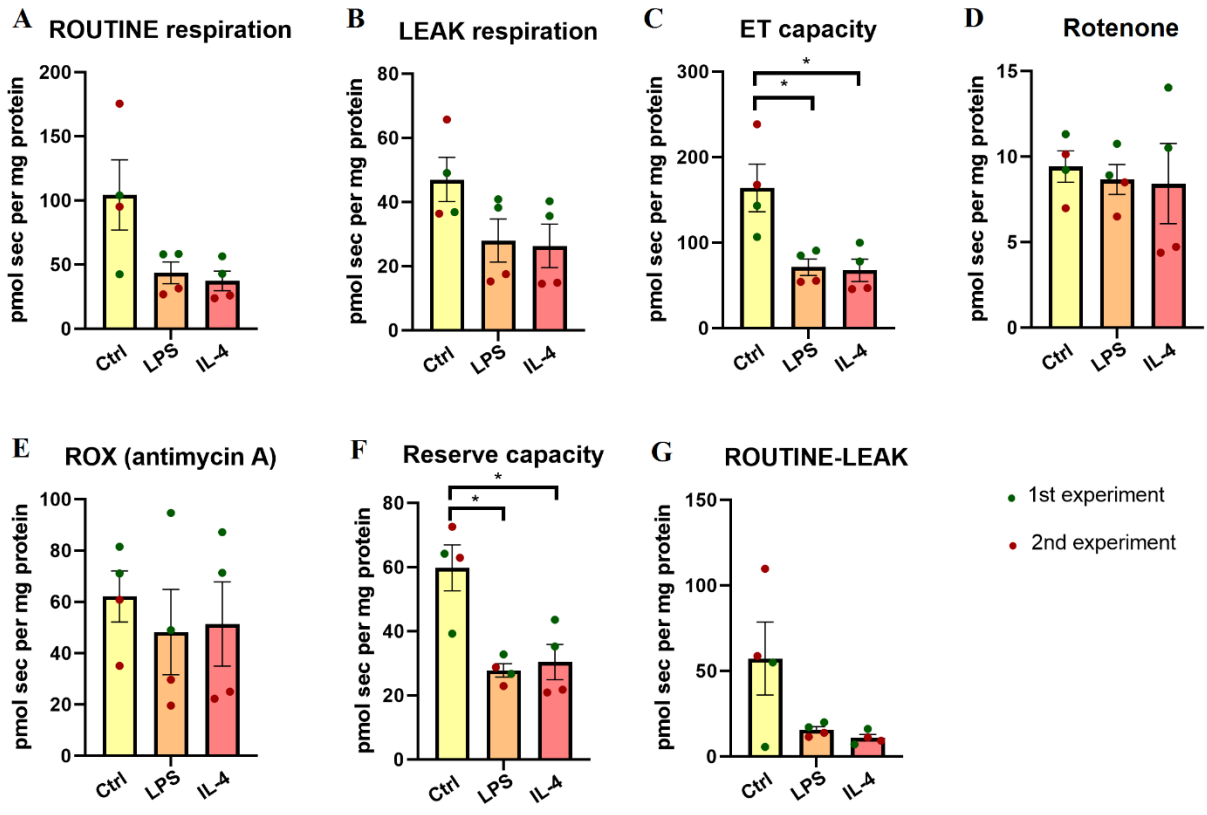

Figure 10: States of mitochondrial respiration in RAW 264.7 cells after LPS and IL-4 treatment and in non-treated controls. ROUTINE respiration (A) and LEAK respiration (B). Electron transfer (ET) capacity (C). Residual oxygen consumption (ROX) after titration of rotenone (complex I inhibitor) and antimycin A (complex III inhibitor) (D and E). Reserve capacity is the ET capacity subtracted by ROUTINE respiration (F). ROUTINE respiration corrected by LEAK respiration (G) is the coupled respiration that shows net OXPHOS capacity – ATP production. Presented results come from two independent experiments (green and red dots). Results are presented as mean values and ± SEM; * p-value < 0.05.

To express respiration independent of cell count, flux control ratios normalized for ET capacity were used as an internal normalization (**Figure 11**). Results show no significant increase or decrease in R/E control ratio or L/E coupling-control ratio in the LPS/IL-4 treated RAW 264.7 cells (**Figure 11A,B**). ROX normalized for ET capacity shows a significant increase in the LPS-treated cells after rotenone titration (**Figure 11C**), while ROX normalized for ET after antimycin A titration does not show any significant difference between control group and treated cells (**Figure 11D**).

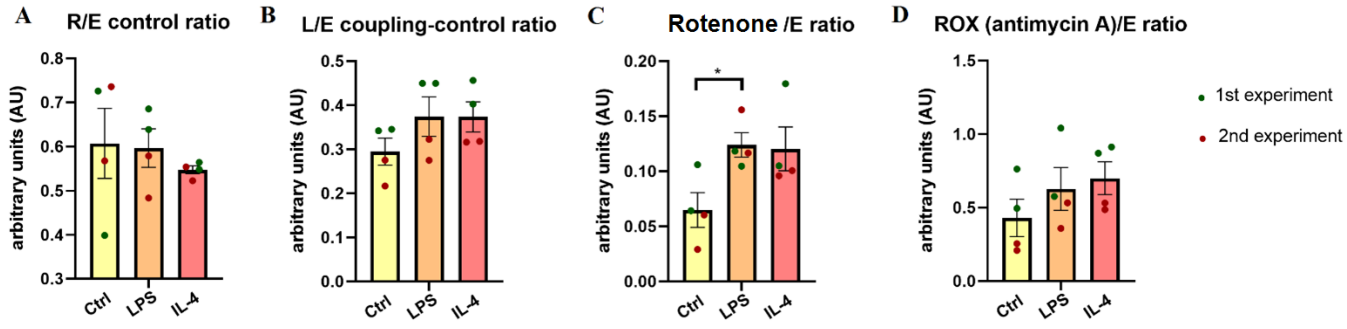

Figure 11: Data from high resolution respirometry of RAW 265.7 cells after LPS/IL-4 treatment normalized for ET capacity. R/E control ratio expresses how close ROUTINE respiration operates to ET capacity (A). L/E coupling-control ratio is an index of uncoupling or dyscoupling at constant ET capacity (B). Figure represents also ROX after rotenone and antimycin A titration normalized for ET capacity (C and D). Presented results come from two independent experiments (green and red dots). Results are presented as mean values and ± SEM; * p-value < 0.05.

3.3 Palmitate treatment does not induce expression of PLA2G7 or DHRS9 in RAW 264.7 cells

To investigate if FAs have influence on levels of PLA2G7 and DHRS9 expression, we performed palmitate (PA) treatment on RAW 264.7 cells. The results from mRNA analysis of RAW 264.7 cells after PA treatment do not show increased expression of PLA2G7 or DHRS9. In fact, the results for PLA2G7 were not detected (undetermined), meaning that the expression of this gene is immensely low, even after PA treatment. DHRS9 expression is slightly induced after treatment with 0.3 mM PA compared to the control group, but the increase is not significant (**Figure 12A**). Additionally, the expression of TNF and CCL2 was measured (**Figure 12B**). Treatment with 0.3 mM PA significantly increased expression of CCL2 comparing to non-treated controls. All the results come from two independent experiments and are normalized with PPIA (housekeeping gene). Due to the low abundance

of PLA2G7, we decided to measure PLA2G7 expression also in non-diluted samples (**Figure S2**). The expression was detectable, although still very low and due to lack of dilution, ΔCq was calculated.

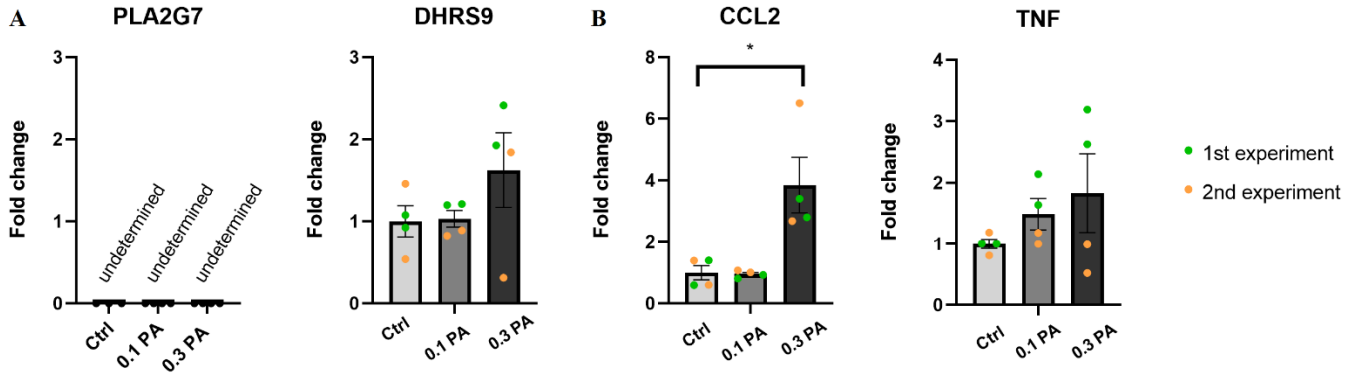

Figure 12: Measurement of expression of PLA2G7, DHRS9 (A), CCL2 and TNF (B) in cDNA from RAW 264.7 cells with (0.1PA and 0.3PA) and without palmitate treatment (Ctrl). Presented results come from two independent experiments (green and orange dots). All the results are normalized with PPIA (housekeeping gene). Results show mean values and ± SEM; * p-value < 0.05.

3.4 Expression of PLA2G7 and DHRS9 in RAW 264.7 cells is induced after LPS/IL-4 treatment

Since PA treatment did induce expression of PLA2G7 or DHRS9, LPS/IL-4 treatment was performed on RAW 264.7 cells to study whether target genes respond to inflammatory stimuli. Expression of following genes was measured with the use of rt qPCR: PLA2G7, DHRS9, CCL2, TNF and ARG1. Results presented below include also validation of shRNA-mediated PLA2G7 knockdown.

3.4.1 PLA2G7 is induced after LPS/IL-4 treatment in RAW 264.7 cells

Since PLA2G7 was not detected in previous qPCR measurement (see previous section) it was decided to carry out validation of shRNA-mediated knockdown of PLA2G7 in non-diluted samples (1:1). Cells with shRNA-mediated knockdown were divided as follows: non treated cells (sh-PLA2G7 Ctrl), cells treated with LPS/IL-4 (sh-PLA2G7 LPS/ sh-PLA2G7 IL-4). SCR shRNA was used as a control and this group was divided into following subgroups: non treated cells (shSCR Ctrl), cells treated with LPS/IL-4 (shSCR LPS/ shSCR IL-4). The data are presented as 2-ΔΔCt in **Figure 13**. The expression of sh-PLA2G7 Ctrl is significantly

lower than in SCR shRNA Ctrl, meaning that the PLA2G7 knockdown was successful. The expression of PLA2G7 is significantly higher in shSCR LPS cells than in shPLA2G7 LPS group, showing that LPS induces PLA2G7 expression in RAW 264.7 cells. Additionally, IL-4 treatment also increased expression in shSCR cells compared to sh-PLA2G7 IL-4 group. Combined, these results indicate that PLA2G7 is induced after LPS and IL-4 stimulation.

More results about macrophages phenotype after PLA2G7 silencing are not presented here due to time constrains but this part will be shown in the master's thesis defence.

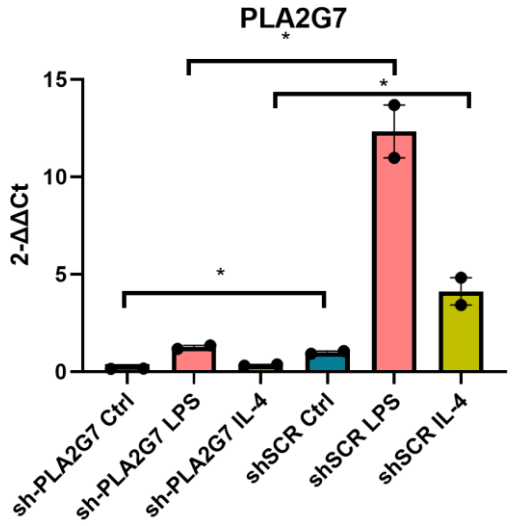

Figure 13: The figure presents data from validation of shRNA-mediated knockdown of PLA2G7 in RAW 264.7 cells. Presented data come from cells with PLA2G7 knockdown (sh-PLA2G7) and are further divided into non-treated group (sh-PLA2G7 Ctrl) and LPS/IL-4 treated groups (sh-PLA2G7 LPS/sh-PLA2G7 IL-4). Second group is shRNA SCR, which serves as a control. shRNA SCR group is further divided into non-treated group (shSCR Ctrl) and LPS/IL-4 treated groups (shSCR LPS/shSCR IL-4). The data from show 2-ΔΔCt values and are presented as mean values and ± SEM; * p-value <0.05.

3.4.2 RAW 264.7 cells treated with LPS/IL-4 show increased expression of DHRS9

Treatment with both LPS and IL-4 resulted in induced DHRS9 (**Figure 14A**). Expression of CCL2 was significantly increased after IL-4 treatment comparing to non-treated control group (**Figure 14B**), while TNF expression increased after LPS treatment (**Figure 14C**). Due to low abundance of ARG1, standard curve for this gene was not obtained (undetermined). Therefore, the data presented in **Figure 14D** show ΔCq values and ARG1 is clearly induced after the IL-4 treatment in RAW 264.7 cells.

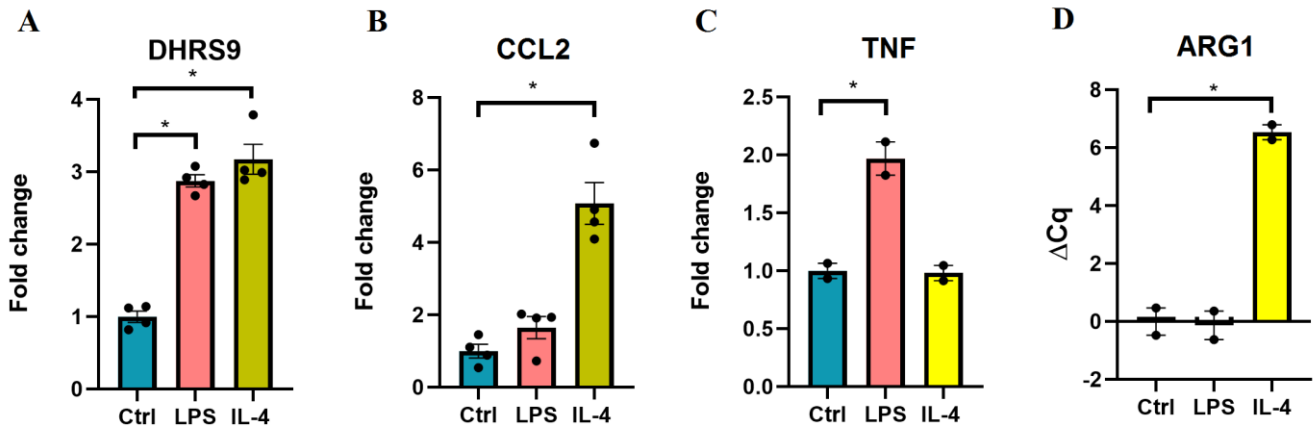

Figure 14: Expression of DHRS9 (A), CCL2 (B), TNF (C) and ARG1 (D) in RAW 264.7 cells after LPS and IL-4 treatment compared to control group. Note that values for ARG1 expression are presented as ΔCq, in contrast to the rest presented as fold change. The figure shows mean values and ± SEM; * p-value < 0.05.

3.5 LPS/IL-4 stimulation combined with palmitate treatment induces DHRS9, but not PLA2G7.

To investigate further, we decided to combine two of the treatments that had been carried out previously (see section 3.3 and 3.4). Hence, RAW 264.7 cells were treated with PA combined with LPS (LPS+0.3PA) or IL-4 (IL-4+0.3PA), and only 0.3 mM PA. The expression of PLA2G7, ARG1, DHRS9, CCL2 and TNF was measured with the use of qPCR. The data are presented in **Figure 15**. Expression of PLA2G7 and ARG1 is presented as ΔCq and the values are not normalized by PPIA (housekeeping gene) due to the lack of standard curve. PLA2G7 was not induced by any of the combined treatments, while ARG1 is clearly induced by the IL-4+0.3PA treatment (**Figure 15A,B**). DHRS9 expression increased significantly after LPS+0.3PA and IL-4+0.3PA co-treatments, with higher values after LPS+0.3PA stimulation (**Figure 15C**). Both CCL2 and TNF were induced after LPS+0.3PA stimulation, but not after any other treatment **(Figure 15D,E**).

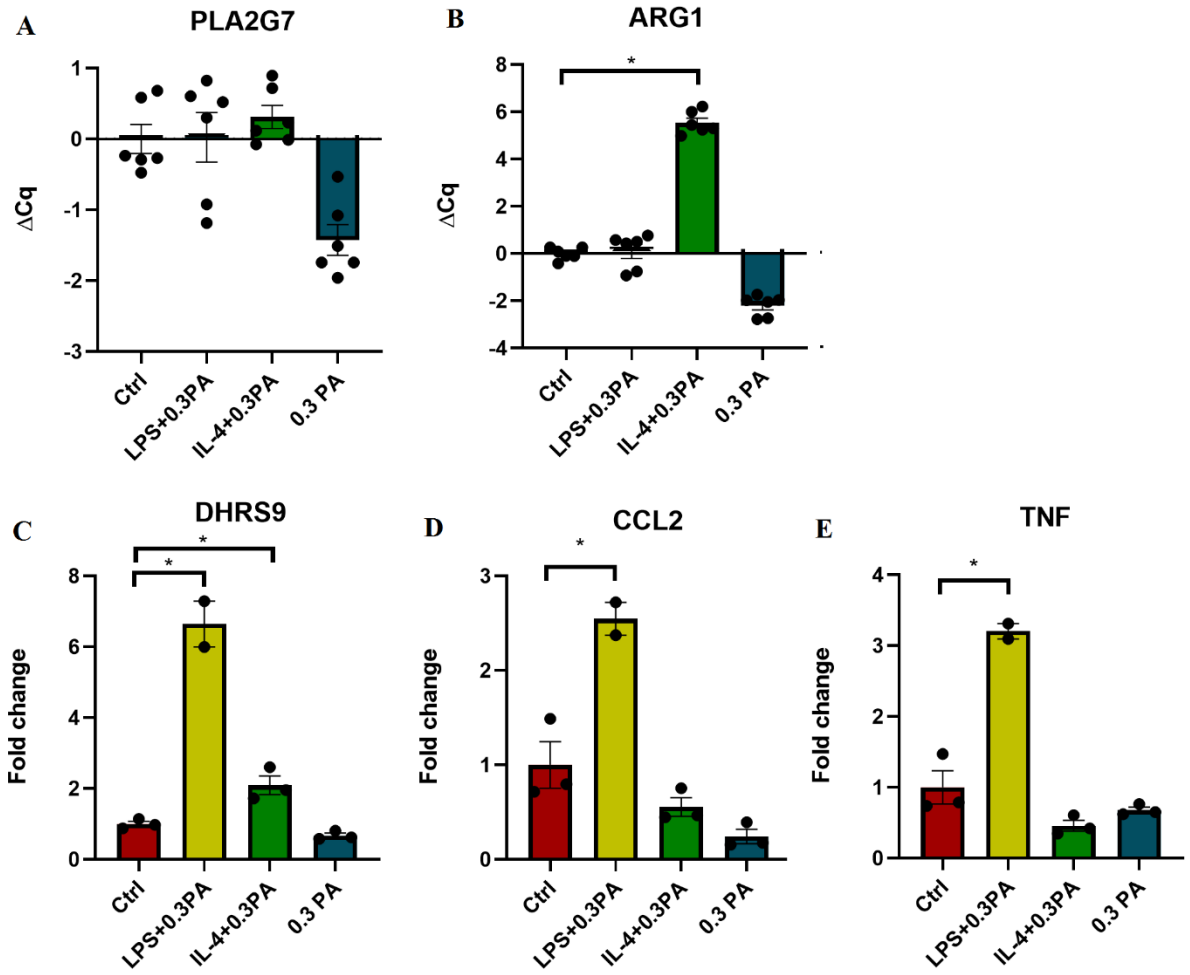

Figure 15: Expression of PLA2G7 (A), ARG1 (B), DHRS9 (C), CCL2 (D) and TNF (E) in RAW 264.7 cells divided into following groups: controls, after LPS/IL-4 treatment combined with 0.3 mM palmitate, and 0.3 mM palmitate treatment. The values for PLA2G7 and ARG1 are presented in ΔCq due to the lack of standard curve for PLA2G7 and ARG1. The figure shows mean values and ± SEM; * p-value < 0.05.

3.6 Culturing of bone marrow derived monocytes from lean and obese mice as an approach to assess expression of selected target genes

To expand our investigation of possible roles of DHRS9 and PLA2G7 in immunometabolism, we decided to obtain bone marrow derived monocytes (BMDMs) from mice (groups: see section 2.6). This way we could enrich this project with gene expression data of PLA2G7 and DHRS9 in animal model (in vivo) in addition to the results from RAW 264.7 cell line. The idea was also to use high resolution respirometry to investigate mitochondrial function in BMDMs.

After extraction of BMDMs, living cells were seen under the microscope, but most of them were not attached to the plate. Therefore, most of the cells were lost during changing of growth media. RNA isolation of the BMDMs was performed, but the RNA concentration was not sufficient for further experiments. Due to that the data for expression of target genes could not be assessed.

4 Discussion

The interplay between ATMs, adipocytes and mitochondria metabolism is currently a topic of many research studies aiming to explore the role of metabolism and particular metabolites in this interplay and ultimately improve obesity-associated disorders. In this project, two genes were investigated in the context of obesity, with a goal of deciphering the role they might play in immunometabolism. Additionally, mitochondria function of mouse macrophage-like cell line under various conditions was explored. Here, we describe for the first time that PLA2G7 and DHRS9 gene expression is elevated in ATMs infiltrated sWAT compared to ATMs resident in vWAT from patients with obesity. We also present these two genes are induced in WAT from humans or mice with obesity.

Literature does not provide much evidence of possible role of DHRS9 in obesity and immunometabolism. However, a recent study shed some light on possible connection between DHRS9 and inflammation. It was reported that DHRS9 exhibits robust oxidative activity toward oxylipins which are a group of FA metabolites involved in several biological processes, including inflammation. It has also been suggested that DHRS9 might be involved in metabolism of leutokriene B4 which is a potent lipid inflammatory mediator secreted by neutrophils and macrophages (75). This might indicate a connection between induced DHRS9 in WAT in obesity and its association with inflammation processes. In RAW 264.7 cells, DHRS9 was induced both after LPS and IL-4 treatment, what might suggest a potential role in inflammatory signalling. Additionally, a co-treatment that combined palmitate with LPS or IL-4 also induced DHRS9. Our results are in agreement with another study that shows an increase of DHRS9 expression after IL-4 treatment (67). In this thesis time limitation hindered attempt at silencing DHRS9 gene. Thus, experiments on DHRS9 knockdown (in RAW 264.7 cells and/or *in vivo*) would be considered an interesting future approach.

Regarding PLA2G7, as mentioned previously, it seems that Lp-PLA_2 (coded by PLA2G7) might be of a dual nature with both beneficial and detrimental effects (see section 1.7.1). Oxidized FA generated by Lp-PLA_2, can exhibit pro- and anti-inflammatory activities (64) and the role of Lp-PLA_2 in atherosclerosis is still under investigation. PLA2G7 was recently found to be a potential therapeutic target for atherosclerosis due to its hypomethylation in symptomatic plaques (76). Bearing in mind that obesity is tightly linked to inflammation and atherosclerosis, it makes our findings about overexpression of PLA2G7 in obese individuals relevant considering immunometabolism. Moreover, it has been established that levels of circulating Lp-PLA_2 seem to be influenced by unfavourable lipid profiles seen in T2D. The same study determined that human adipocytes might contribute as a source of Lp-PLA_2 (77). Interestingly, Ferguson et al showed that Lp-PL_2 levels differ depending on macrophages polarization. Lp-PLA_2 increased slightly during polarization to M1 macrophages but declined during polarization towards M2 (78). M1 macrophages are classically activated through LPS (among others). However, as reviewed by Huang et al, *in vivo* and *in vitro* experiments show contradictory results regarding expression of Lp-PLA_2 after LPS stimulation (79). For example, the human study conducted by Ferguson et al, Lp-PLA_2 has not shown an increased mRNA expression after LPS stimulation (in whole-blood samples) (78). Yet, experiments conducted on RAW 264.7 cell line established that LPS induced transcriptional activation of Lp-PLA_2 (80). It indicates that the differences between RAW 264.7 cell line and human samples might play a role in the outcome of performed experiments and should be considered as a limitation of this project. In our study, we did not determine whether ATMs are the main source of PLA2G7 in adipose tissue, but we showed that this gene is specifically induced in this immune cell infiltrated in sWAT compared to vWAT besides of whole AT. It suggests that macrophages might be an important source of PLA2G7, or at least, a recognized contributor to the regulation of this gene. It is also important to mention that PLA2G7 is a part of arachidonic acid pathway. Lp-PLA_2 can be activated through Toll-like-receptor stimulation and its activation leads to the release of arachidonic acid from plasma membrane. Arachidonic acid further converts to eicosanoids including prostaglandins which are known for their involvement in inflammation processes (81-83). A very recent study published in a prestigious journal Science revealed that knock-down of PLA2G7 in mice leads to lower levels of inflammasome proteins in KO-PLA2G7 mice fed HFD. What is more, a loss of PLA2G7 resulted in lower abundance of B cells, T cells and macrophage subsets which impair adipose metabolism. The knock-down led to an increased abundance of macrophages with more anti-inflammatory phenotype. Results of this study suggest that in AT

microenvironment PLA2G7 might function as inflammasome regulator (84). Since we focused on ATM in humans, we did not examine whether other macrophages or monocytes could be expressing PLA2G7 in obesity. We attempted to isolate bone marrow macrophages from mice, but without success in our *in vitro* experiments. However, our results from RAW 264.7 cells clearly indicate that PLA2G7 is induced after LPS and (to some degree) after IL-4 stimulation. We have also investigated expression of PLA2G7 in RAW 264.7 cells after combined treatment (palmitate with LPS or IL-4). The outcome of this experiment does not show any increase in PLA2G7 expression after this type of stimulation. Due to the limited time and substantial delay in shipments of essential products, we could not extend our investigation of RAW 264.7 cells with PLA2G7 knockdown. Results from examination of macrophage phenotypes in the PLA2G7 knockdown cells are going to be obtained later and presented only at the defence (oral presentation) of this thesis.

Pro-inflammatory mediators are being generated through the Lp-PLA_2 mediated hydrolysis of ox-LDL (79). As mentioned before (see section 1.6), when the levels of ox-LDL are too high for macrophages to cope with, they become foam cells. It has been established that levels of Lp-PLA_2 are higher in foam cells than in mature macrophages (78). Also, a study by Kadl et al (85) proposed a new type of macrophages termed Mox. Mox macrophages play a role in atherosclerotic lesion development and in chronic inflammation. This type has a gene expression pattern quite different from M1 and M2 macrophages. Phospholipid oxidation products that accumulate in atherosclerotic lesions were found to have an impact on the Mox phenotype (85). Other group demonstrated that ATMs can also develop a different phenotype and described it as 'metabolically-activated' (MMe) macrophages. Saturated FFAs are believed to be a key activator of this phenotype. MMe macrophages are of bilateral nature: on the one side secreted cytokines result in detrimental effect, and on the other side lysosomal exocytosis to dead adipocytes gives a beneficial function (86). The variations in phenotypes of ATMs might be one of the limitations of the experiments performed in this study. Also, it should be kept in mind that most of the results presented in this thesis come from RAW 264.7 cell line and it can also be considered a limitation. Ideally, this thesis would have included gene expression data from BMDMs of mice (lean vs obese), but this approach has not been successful. Moreover, detection and investigation of PLA2G7 might have been easier in foam cells comparing to RAW 264.7 cells.

Interactions between mitochondria and macrophages are topic of many reviews (87-89). However, many of them focus on the involvement of metabolic pathways and various

metabolites and their impact on macrophage polarization or immune cells activation. In this project we focused on concrete states of mitochondrial respiration and the possible influence of palmitate and LPS/IL-4 treatment on mouse macrophage-like RAW 264.7 cells. Bossche et al presented that in mouse bone-marrow derived macrophages LPS-treated macrophages (M1 macrophages), OXPHOS was significantly suppressed, compared to naïve macrophages (90). Another study showed a similar outcome where maximal oxidative metabolism in BMDMs from mice was highly reduced in LPS-treated bone marrow-derived macrophages. Moreover, BMDMs treated with LPS showed no reserve capacity (91). Scrima et al analysed RAW 264.7 under various conditions and also observed decreased values after FCCP titration (decreased ET capacity) in the LPS-treated group (92). This data coincides with our findings which show that LPS treatment significantly decreases ET capacity and reserve capacity in RAW 264.7 cells. This indicates that LPS treatment favours differentiation of RAW 264.7 cells into a M1 macrophages phenotype characterized by low oxidative potential and high glycolytic activity (56, 93). However, it seems that our data from IL-4 treated cells differ from the results obtained in previously mentioned publications (90, 91), where it was demonstrated that IL-4 stimulation enhances oxidative metabolism and is characterized by high reserve capacity. Our analysis indicates that IL-4 stimulation in RAW 264.7 cells gives similar outcome as LPS stimulation – decreased ET capacity and reserve capacity. To verify whether our IL-4 treatment was efficient and worked correctly, we examined ARG1 expression using rt qPCR. ARG1 is a marker for M2 macrophages, and its expression levels were significantly elevated in the IL-4 treated cells. The expression of ARG1 confirms that the IL-4 treatment on RAW 264.7 cells worked as expected, suggesting that the outcome of our high resolution respirometry analysis reveals data that have not been shown before. Interestingly, several studies have reported that glycolysis, might be closer connected to M2 macrophages metabolism than previously considered. IL-4 together with other stimuli seemed to contribute to the upregulation in glycolysis in M2 phenotype (94). We might speculate that this similarity between metabolic pathways used by M1 and M2 macrophages could partially explain similarities between our results after LPS and IL-4 stimulation. However, rewiring of metabolism in macrophages is still under investigation, with a recent article pointing out that it might be time dependent. In their publication, Seim and Fan present how LPS stimulation alters Krebs cycle during macrophage activation. It appears that in very early stages of macrophage activation through LPS, OXPHOS is in fact enhanced (89). Therefore, we should consider that remodelling of Krebs cycle is time dependent and M1 and M2 polarization does

not increase solely glycolysis and OXPHOS, respectively. It also shows challenges that are associated with analysing mitochondrial respiration in macrophages.

It has been established and reviewed that FFAs might cause inflammatory reactions in macrophages or have an influence on insulin resistance (49, 95). Therefore, our further investigation of states of mitochondrial respiration in RAW 264.7 macrophages included high resolution respirometry analysis after treating the cells with palmitate. There is little knowledge on this topic, and it has not been much investigated in any macrophage-like cell line. Therefore, the results presented in this thesis might be an interesting contribution to the current studies in this field. Our data present a significant increase of residual oxygen consumption in RAW 264.7 cells after 24h 0.3mM palmitate treatment. This might suggest that palmitate is able to alter metabolic pathways so that after PA stimulation the cells change their source of energy production. A recent study investigated palmitate's influence on hepatoma cells and established that the treatment enhanced glycolysis. It was also revealed that redox signalling was altered by palmitate, but there was no focus on residual oxygen consumption. It only shows that this subject is under current investigation and that there is a clear involvement of palmitate overload and lipotoxicity on mitochondrial metabolism (96). We might speculate that the factor responsible for the increased residual oxygen consumption in the treated cells are NADPH oxidases (NOXs). NOXs are expressed in macrophages and are involved in inflammation reactions and part of residual oxygen consumption. This could indicate a link between overload of fatty acids and increased NOXs' activity which could be further connected to the interplay between obesity and inflammation. Interestingly, a recent investigation on RAW 264.7 macrophages showed that NADPH oxidase 4 (NOX4) expression increased after a treatment that combined palmitate and LPS (97). Such findings make various macrophage stimulation an interesting future approach for high resolution respirometry experiments.

A valuable contribution to our results from high resolution respirometry would be an analysis of BMDMs from mice but, as mentioned previously, we did not obtain enough cells while culturing. Due to the limited time for this project, we have not analysed whether knockdown of PLA2G7 changes subsequent stages of mitochondrial respiration, but it would be considered as one of the next steps of the investigation. In fact, a recent review focused on how mitochondria orchestrate macrophages function in atherosclerotic plaques (98). This would be especially interesting to study in the context of PLA2G7 expression. It is important to mention that our experiments were performed using three Oroboros® oxygraphs which

corresponds with six analysis-chambers in total. Due to that, we had to perform two separate experiments to acquire enough data. Preferably, we would have performed additional experiments to make our data more reliable.

5 Conclusions

The execution of this project led us to the following conclusions:

- PLA2G7 and DHRS9 are overexpressed in ATMs from sWAT compared to vWAT in the individuals with obesity, showing that expression of these genes in ATMs is modulated depending on fat depot.
- PLA2G7 and DHRS9 are induced in WAT in mice fed high fat diet and in humans with obesity compared to normal-weight controls.

Our experiments on RAW 264.7 mouse macrophage-like cell line indicate that:

- PLA2G7 and DHRS9 are induced after LPS stimulation, but not after palmitate treatment. Expression of DHRS9 is also induced after IL-4 stimulation.

Investigation of states of mitochondrial respiration in RAW 264.7 cells showed that:

- Palmitate treatment induces residual oxygen consumption in this cell line, while LPS and IL-4 stimulation worsens oxidative phosphorylation.

Together, these conclusions open a very important window for the study of PLA2G7 and DHRS9 as novel therapeutics targets involved in energy metabolism and inflammatory processes in obesity.

6 References

1. Mayoral LP, Andrade GM, Mayoral EP, Huerta TH, Canseco SP, Rodal Canales FJ, et al. Obesity subtypes, related biomarkers & heterogeneity. Indian J Med Res. 2020;151(1):11-21.
2. World Health Organization. Obesity and overweight. 2021.
3. Smith KB, Smith MS. Obesity Statistics. Primary Care: Clinics in Office Practice. 2016;43(1):121-35.
4. Hauner H. Managing type 2 diabetes mellitus in patients with obesity. Treat Endocrinol. 2004;3(4):223-32.
5. Yazıcı D, Sezer H. Insulin Resistance, Obesity and Lipotoxicity. Adv Exp Med Biol. 2017;960:277-304.
6. Pulgaron ER, Delamater AM. Obesity and type 2 diabetes in children: epidemiology and treatment. Curr Diab Rep. 2014;14(8):508.
7. World Health Organization. Diabetes. 2021.
8. Kelly T, Yang W, Chen CS, Reynolds K, He J. Global burden of obesity in 2005 and projections to 2030. International Journal of Obesity. 2008;32(9):1431-7.
9. Zhou Y, Chi J, Lv W, Wang Y. Obesity and diabetes as high-risk factors for severe coronavirus disease 2019 (Covid-19). Diabetes Metab Res Rev. 2021;37(2):e3377.
10. Song T, Kuang S. Adipocyte dedifferentiation in health and diseases. Clin Sci (Lond). 2019;133(20):2107-19.
11. Tang QQ, Lane MD. Adipogenesis: from stem cell to adipocyte. Annu Rev Biochem. 2012;81:715-36.
12. Bora P, Majumdar AS. Adipose tissue-derived stromal vascular fraction in regenerative medicine: a brief review on biology and translation. Stem Cell Res Ther. 2017;8(1):145.
13. Zwick RK, Guerrero-Juarez CF, Horsley V, Plikus MV. Anatomical, Physiological, and Functional Diversity of Adipose Tissue. Cell Metabolism. 2018;27(1):68-83.
14. Cedikova M, Kripnerová M, Dvorakova J, Pitule P, Grundmanova M, Babuska V, et al. Mitochondria in White, Brown, and Beige Adipocytes. Stem Cells Int. 2016;2016:6067349.
15. Thomas EL, Saeed N, Hajnal JV, Brynes A, Goldstone AP, Frost G, et al. Magnetic resonance imaging of total body fat. Journal of Applied Physiology. 1998;85(5):1778-85.
16. Bielczyk-Maczynska E. White Adipocyte Plasticity in Physiology and Disease. Cells. 2019;8(12).
17. Sethi JK, Vidal-Puig AJ. Thematic review series: Adipocyte Biology. Adipose tissue function and plasticity orchestrate nutritional adaptation. Journal of Lipid Research. 2007;48(6):1253-62.
18. Després JP. Is visceral obesity the cause of the metabolic syndrome? Ann Med. 2006;38(1):52-63.
19. Wajchenberg BL, Giannella-Neto D, da Silva MER, Santos RF. Depot-Specific Hormonal Characteristics of Subcutaneous and Visceral Adipose Tissue and their Relation to the Metabolic Syndrome. Horm Metab Res. 2002;34(11/12):616-21.
20. Sun K, Kusminski CM, Scherer PE. Adipose tissue remodeling and obesity. The Journal of Clinical Investigation. 2011;121(6):2094-101.
21. Wang QA, Tao C, Gupta RK, Scherer PE. Tracking adipogenesis during white adipose tissue development, expansion and regeneration. Nature Medicine. 2013;19(10):1338-44.
22. Pellegrinelli V, Carobbio S, Vidal-Puig A. Adipose tissue plasticity: how fat depots respond differently to pathophysiological cues. Diabetologia. 2016;59(6):1075-88.
23. Kershaw EE, Flier JS. Adipose Tissue as an Endocrine Organ. The Journal of Clinical Endocrinology & Metabolism. 2004;89(6):2548-56.
24. Frayn KN, Karpe F, Fielding BA, Macdonald IA, Coppack SW. Integrative physiology of human adipose tissue. International Journal of Obesity. 2003;27(8):875-88.
25. Wernstedt Asterholm I, Tao C, Morley Thomas S, Wang Qiong A, Delgado-Lopez F, Wang Zhao V, et al. Adipocyte Inflammation Is Essential for Healthy Adipose Tissue Expansion and Remodeling. Cell Metabolism. 2014;20(1):103-18.

26. Leuti A, Fazio D, Fava M, Piccoli A, Oddi S, Maccarrone M. Bioactive lipids, inflammation and chronic diseases. Advanced Drug Delivery Reviews. 2020;159:133-69.
27. Hotamisligil GS. Inflammation and metabolic disorders. Nature. 2006;444(7121):860-7.
28. Li C, Xu MM, Wang K, Adler AJ, Vella AT, Zhou B. Macrophage polarization and meta-inflammation. Translational Research. 2018;191:29-44.
29. Lumeng CN, Saltiel AR. Inflammatory links between obesity and metabolic disease. The Journal of Clinical Investigation. 2011;121(6):2111-7.
30. Saltiel AR, Olefsky JM. Inflammatory mechanisms linking obesity and metabolic disease. J Clin Invest. 2017;127(1):1-4.
31. Muir LA, Neeley CK, Meyer KA, Baker NA, Brosius AM, Washabaugh AR, et al. Adipose tissue fibrosis, hypertrophy, and hyperplasia: Correlations with diabetes in human obesity. Obesity. 2016;24(3):597-605.
32. Grant RW, Dixit VD. Adipose tissue as an immunological organ. Obesity (Silver Spring). 2015;23(3):512-8.
33. Hotamisligil GS, Arner P, Caro JF, Atkinson RL, Spiegelman BM. Increased adipose tissue expression of tumor necrosis factor-alpha in human obesity and insulin resistance. J Clin Invest. 1995;95(5):2409-15.
34. Schoettl T, Fischer IP, Ussar S. Heterogeneity of adipose tissue in development and metabolic function. Journal of Experimental Biology. 2018;221(Suppl_1).
35. Weisberg SP, McCann D, Desai M, Rosenbaum M, Leibel RL, Ferrante AW, Jr. Obesity is associated with macrophage accumulation in adipose tissue. J Clin Invest. 2003;112(12):1796-808.
36. Kunz HE, Hart CR, Gries KJ, Parvizi M, Laurenti M, Dalla Man C, et al. Adipose tissue macrophage populations and inflammation are associated with systemic inflammation and insulin resistance in obesity. Am J Physiol Endocrinol Metab. 2021;321(1):E105-e21.
37. Lee J. Adipose tissue macrophages in the development of obesity-induced inflammation, insulin resistance and type 2 diabetes. Archives of pharmacal research. 2013;36(2):208-22.
38. Gordon S, Taylor PR. Monocyte and macrophage heterogeneity. Nat Rev Immunol. 2005;5(12):953-64.
39. Mosser DM, Edwards JP. Exploring the full spectrum of macrophage activation. Nat Rev Immunol. 2008;8(12):958-69.
40. Chinetti-Gbaguidi G, Staels B. Macrophage polarization in metabolic disorders: functions and regulation. Curr Opin Lipidol. 2011;22(5):365-72.
41. Martinez FO, Sica A, Mantovani A, Locati M. Macrophage activation and polarization. Front Biosci. 2008;13:453-61.
42. Lumeng CN, DelProposto JB, Westcott DJ, Saltiel AR. Phenotypic switching of adipose tissue macrophages with obesity is generated by spatiotemporal differences in macrophage subtypes. Diabetes. 2008;57(12):3239-46.
43. Lumeng CN, Bodzin JL, Saltiel AR. Obesity induces a phenotypic switch in adipose tissue macrophage polarization. J Clin Invest. 2007;117(1):175-84.
44. Zeyda M, Farmer D, Todoric J, Aszmann O, Speiser M, Györi G, et al. Human adipose tissue macrophages are of an anti-inflammatory phenotype but capable of excessive pro-inflammatory mediator production. Int J Obes (Lond). 2007;31(9):1420-8.
45. Wang X, Cao Q, Yu L, Shi H, Xue B, Shi H. Epigenetic regulation of macrophage polarization and inflammation by DNA methylation in obesity. JCI Insight. 2016;1(19):e87748.
46. Young SG, Zechner R. Biochemistry and pathophysiology of intravascular and intracellular lipolysis. Genes Dev. 2013;27(5):459-84.
47. Zechner R, Zimmermann R, Eichmann TO, Kohlwein SD, Haemmerle G, Lass A, et al. FAT SIGNALS--lipases and lipolysis in lipid metabolism and signaling. Cell Metab. 2012;15(3):279-91.
48. Engin AB. What Is Lipotoxicity? In: Engin AB, Engin A, editors. Obesity and Lipotoxicity. Cham: Springer International Publishing; 2017. p. 197-220.
49. Prieur X, Roszer T, Ricote M. Lipotoxicity in macrophages: evidence from diseases associated with the metabolic syndrome. Biochim Biophys Acta. 2010;1801(3):327-37.

50. Cao H, Jia Q, Yan L, Chen C, Xing S, Shen D. Quercetin Suppresses the Progression of Atherosclerosis by Regulating MST1-Mediated Autophagy in ox-LDL-Induced RAW264.7 Macrophage Foam Cells. Int J Mol Sci. 2019;20(23).
51. Angajala A, Lim S, Phillips JB, Kim J-H, Yates C, You Z, et al. Diverse Roles of Mitochondria in Immune Responses: Novel Insights Into Immuno-Metabolism. Frontiers in Immunology. 2018;9.
52. Nassef MZ, Hanke JE, Hiller K. Mitochondrial metabolism in macrophages. Am J Physiol Cell Physiol. 2021;321(6):C1070-c81.
53. Mills EL, O'Neill LA. Reprogramming mitochondrial metabolism in macrophages as an anti-inflammatory signal. Eur J Immunol. 2016;46(1):13-21.
54. Griffiths HR, Gao D, Pararasa C. Redox regulation in metabolic programming and inflammation. Redox Biol. 2017;12:50-7.
55. Brestoff JR, Wilen CB, Moley JR, Li Y, Zou W, Malvin NP, et al. Intercellular Mitochondria Transfer to Macrophages Regulates White Adipose Tissue Homeostasis and Is Impaired in Obesity. Cell Metab. 2021;33(2):270-82.e8.
56. Wang Y, Tang B, Long L, Luo P, Xiang W, Li X, et al. Improvement of obesity-associated disorders by a small-molecule drug targeting mitochondria of adipose tissue macrophages. Nature Communications. 2021;12(1):102.
57. Loos RJF, Yeo GSH. The genetics of obesity: from discovery to biology. Nature Reviews Genetics. 2022;23(2):120-33.
58. Lu Z, Meng L, Sun Z, Shi X, Shao W, Zheng Y, et al. Differentially Expressed Genes and Enriched Signaling Pathways in the Adipose Tissue of Obese People. Frontiers in Genetics. 2021;12.
59. McConnell JP, Hoefner DM. Lipoprotein-associated phospholipase A2. Clin Lab Med. 2006;26(3):679-97, vii.
60. Grallert H, Dupuis J, Bis JC, Dehghan A, Barbalic M, Baumert J, et al. Eight genetic loci associated with variation in lipoprotein-associated phospholipase A2 mass and activity and coronary heart disease: meta-analysis of genome-wide association studies from five community-based studies. Eur Heart J. 2012;33(2):238-51.
61. Stafforini DM, Elstad MR, McIntyre TM, Zimmerman GA, Prescott SM. Human macrophages secret platelet-activating factor acetylhydrolase. J Biol Chem. 1990;265(17):9682-7.
62. Wilensky RL, Macphee CH. Lipoprotein-associated phospholipase A(2) and atherosclerosis. Curr Opin Lipidol. 2009;20(5):415-20.
63. Tellis CC, Tselepis AD. Pathophysiological role and clinical significance of lipoprotein-associated phospholipase A_2 (Lp-PLA_2) bound to LDL and HDL. Curr Pharm Des. 2014;20(40):6256-69.
64. Rosenson RS, Stafforini DM. Modulation of oxidative stress, inflammation, and atherosclerosis by lipoprotein-associated phospholipase A2. J Lipid Res. 2012;53(9):1767-82.
65. Chetyrkin SV, Belyaeva OV, Gough WH, Kedishvili NY. Characterization of a novel type of human microsomal 3alpha -hydroxysteroid dehydrogenase: unique tissue distribution and catalytic properties. J Biol Chem. 2001;276(25):22278-86.
66. Soref CM, Di YP, Hayden L, Zhao YH, Satre MA, Wu R. Characterization of a novel airway epithelial cell-specific short chain alcohol dehydrogenase/reductase gene whose expression is up-regulated by retinoids and is involved in the metabolism of retinol. J Biol Chem. 2001;276(26):24194-202.
67. Riquelme P, Amodio G, Macedo C, Moreau A, Obermajer N, Brochhausen C, et al. DHRS9 Is a Stable Marker of Human Regulatory Macrophages. Transplantation. 2017;101(11):2731-8.
68. Hu L, Chen HY, Han T, Yang GZ, Feng D, Qi CY, et al. Downregulation of DHRS9 expression in colorectal cancer tissues and its prognostic significance. Tumour Biol. 2016;37(1):837-45.
69. Li HB, Zhou J, Zhao F, Yu J, Xu L. Prognostic Impact of DHRS9 Overexpression in Pancreatic Cancer. Cancer Manag Res. 2020;12:5997-6006.
70. Gonzalez-Franquesa A, Gama-Perez P, Kulis M, Dahdah N, Moreno-Gomez S, Latorre-Pellicer A, et al. Obesity causes irreversible mitochondria failure in visceral adipose tissue

despite successful anti-obesogenic lifestyle-based interventions. bioRxiv. 2020:2020.07.08.194167.
71. Schwartz EA, Zhang WY, Karnik SK, Borwege S, Anand VR, Laine PS, et al. Nutrient modification of the innate immune response: a novel mechanism by which saturated fatty acids greatly amplify monocyte inflammation. Arterioscler Thromb Vasc Biol. 2010;30(4):802-8.
72. Gnaiger E. Mitochondrial pathways and respiratory control. An introduction to OXPHOS analysis. 5th ed.: Bioenergetics Communications 2020.2; 2020.
73. Zdrazilova L, Hansikova H, Gnaiger E. Comparable respiratory activity in attached and suspended human fibroblasts. PLOS ONE. 2022;17(3):e0264496.
74. Bidault G, Virtue S, Petkevicius K, Jolin HE, Dugourd A, Guénantin AC, et al. SREBP1-induced fatty acid synthesis depletes macrophages antioxidant defences to promote their alternative activation. Nat Metab. 2021;3(9):1150-62.
75. Belyaeva OV, Wirth SE, Boeglin WE, Karki S, Goggans KR, Wendell SG, et al. Dehydrogenase reductase 9 (SDR9C4) and related homologs recognize a broad spectrum of lipid mediator oxylipins as substrates. J Biol Chem. 2022;298(1):101527.
76. Li J, Zhang X, Yang M, Yang H, Xu N, Fan X, et al. DNA methylome profiling reveals epigenetic regulation of lipoprotein-associated phospholipase A(2) in human vulnerable atherosclerotic plaque. Clin Epigenetics. 2021;13(1):161.
77. Jackisch L, Kumsaiyai W, Moore JD, Al-Daghri N, Kyrou I, Barber TM, et al. Differential expression of Lp-PLA2 in obesity and type 2 diabetes and the influence of lipids. Diabetologia. 2018;61(5):1155-66.
78. Ferguson JF, Hinkle CC, Mehta NN, Bagheri R, Derohannessian SL, Shah R, et al. Translational studies of lipoprotein-associated phospholipase A_2 in inflammation and atherosclerosis. J Am Coll Cardiol. 2012;59(8):764-72.
79. Huang F, Wang K, Shen J. Lipoprotein-associated phospholipase A2: The story continues. Med Res Rev. 2020;40(1):79-134.
80. Wu X, Zimmerman GA, Prescott SM, Stafforini DM. The p38 MAPK pathway mediates transcriptional activation of the plasma platelet-activating factor acetylhydrolase gene in macrophages stimulated with lipopolysaccharide. J Biol Chem. 2004;279(34):36158-65.
81. Vainio P, Gupta S, Ketola K, Mirtti T, Mpindi JP, Kohonen P, et al. Arachidonic acid pathway members PLA2G7, HPGD, EPHX2, and CYP4F8 identified as putative novel therapeutic targets in prostate cancer. Am J Pathol. 2011;178(2):525-36.
82. Norris Paul C, Gosselin D, Reichart D, Glass Christopher K, Dennis Edward A. Phospholipase A2 regulates eicosanoid class switching during inflammasome activation. Proceedings of the National Academy of Sciences. 2014;111(35):12746-51.
83. Diaconu A, Coculescu B-I, Manole G, Vultur H, Coculescu EC, Stocheci CM, et al. Lipoprotein-associated phospholipase A2 (Lp-PLA2) – possible diagnostic and risk biomarker in chronic ischaemic heart disease. Journal of Enzyme Inhibition and Medicinal Chemistry. 2021;36(1):68-73.
84. Spadaro O, Youm Y, Shchukina I, Ryu S, Sidorov S, Ravussin A, et al. Caloric restriction in humans reveals immunometabolic regulators of health span. Science. 2022;375(6581):671-7.
85. Kadl A, Meher AK, Sharma PR, Lee MY, Doran AC, Johnstone SR, et al. Identification of a novel macrophage phenotype that develops in response to atherogenic phospholipids via Nrf2. Circ Res. 2010;107(6):737-46.
86. Coats BR, Schoenfelt KQ, Barbosa-Lorenzi VC, Peris E, Cui C, Hoffman A, et al. Metabolically Activated Adipose Tissue Macrophages Perform Detrimental and Beneficial Functions during Diet-Induced Obesity. Cell Rep. 2017;20(13):3149-61.
87. Wang Y, Li N, Zhang X, Horng T. Mitochondrial metabolism regulates macrophage biology. J Biol Chem. 2021;297(1):100904.
88. Tur J, Vico T, Lloberas J, Zorzano A, Celada A. Macrophages and Mitochondria: A Critical Interplay Between Metabolism, Signaling, and the Functional Activity. Adv Immunol. 2017;133:1-36.
89. Seim GL, Fan J. A matter of time: temporal structure and functional relevance of macrophage metabolic rewiring. Trends Endocrinol Metab. 2022;33(5):345-58.

90. Van den Bossche J, Baardman J, Otto Natasja A, van der Velden S, Neele Annette E, van den Berg Susan M, et al. Mitochondrial Dysfunction Prevents Repolarization of Inflammatory Macrophages. Cell Reports. 2016;17(3):684-96.
91. Van den Bossche J, Baardman J, de Winther MP. Metabolic Characterization of Polarized M1 and M2 Bone Marrow-derived Macrophages Using Real-time Extracellular Flux Analysis. J Vis Exp. 2015(105).
92. Scrima R, Menga M, Pacelli C, Agriesti F, Cela O, Piccoli C, et al. Para-hydroxyphenylpyruvate inhibits the pro-inflammatory stimulation of macrophage preventing LPS-mediated nitro-oxidative unbalance and immunometabolic shift. PLoS One. 2017;12(11):e0188683.
93. Batista-Gonzalez A, Vidal R, Criollo A, Carreño LJ. New Insights on the Role of Lipid Metabolism in the Metabolic Reprogramming of Macrophages. Frontiers in Immunology. 2020;10.
94. Diskin C, Pålsson-McDermott EM. Metabolic Modulation in Macrophage Effector Function. Front Immunol. 2018;9:270.
95. Korbecki J, Bajdak-Rusinek K. The effect of palmitic acid on inflammatory response in macrophages: an overview of molecular mechanisms. Inflamm Res. 2019;68(11):915-32.
96. Kakimoto PA, Serna JDC, de Miranda Ramos V, Zorzano A, Kowaltowski AJ. Increased glycolysis is an early consequence of palmitate lipotoxicity mediated by redox signaling. Redox Biol. 2021;45:102026.
97. Hwangbo H, Ji SY, Kim MY, Kim SY, Lee H, Kim GY, et al. Anti-Inflammatory Effect of Auranofin on Palmitic Acid and LPS-Induced Inflammatory Response by Modulating TLR4 and NOX4-Mediated NF-κB Signaling Pathway in RAW264.7 Macrophages. Int J Mol Sci. 2021;22(11).
98. Dumont A, Lee M, Barouillet T, Murphy A, Yvan-Charvet L. Mitochondria orchestrate macrophage effector functions in atherosclerosis. Molecular Aspects of Medicine. 2021;77:100922.

7 Supplementary materials

Table S1: A list over TaqMan assays used for qPCR in this project.

Gene name	Symbol	TaqMan Assay ID
Peptidyl-prolyl cis-trans isomerase A	PPIA	Mm02342430_g1
Platelet-activating factor acetylhydrolase A2	PLA2G7	Mm00479105_m1
Dehydrogenase/Reductase 9	DHRS9	Mm00615706_m1
C-C Motif Chemokine Ligand 2	CCL2	Mm00441242_m1
Tumor Necrosis Factor	TNF	Mm00443258_m1
Arginase 1	ARG1	Mm00475988_m1

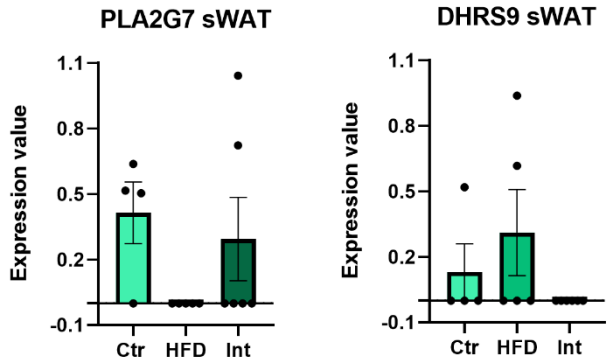

Figure S1: Levels of expression of PLA2G7 and DHRS9 in sWAT from mice. The data are divided into three groups: controls (Ctr, lean mice), high-fat diet fed (HFD, obese mice) and intervention (Int, mice on caloric restriction and exercise after HFD). The figure shows mean and ± SEM values.

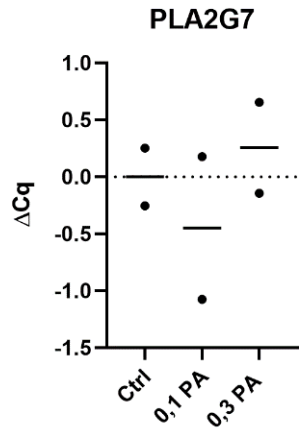

Figure S2: Expression of PLA2G7 in non-diluted samples of cDNA from RAW 264.7 cells treated with 0.1 mM PA (0.1 PA), 0.3 mM PA (0.3 µPA) and non-treated cells (Ctrl). The figure shows mean values.

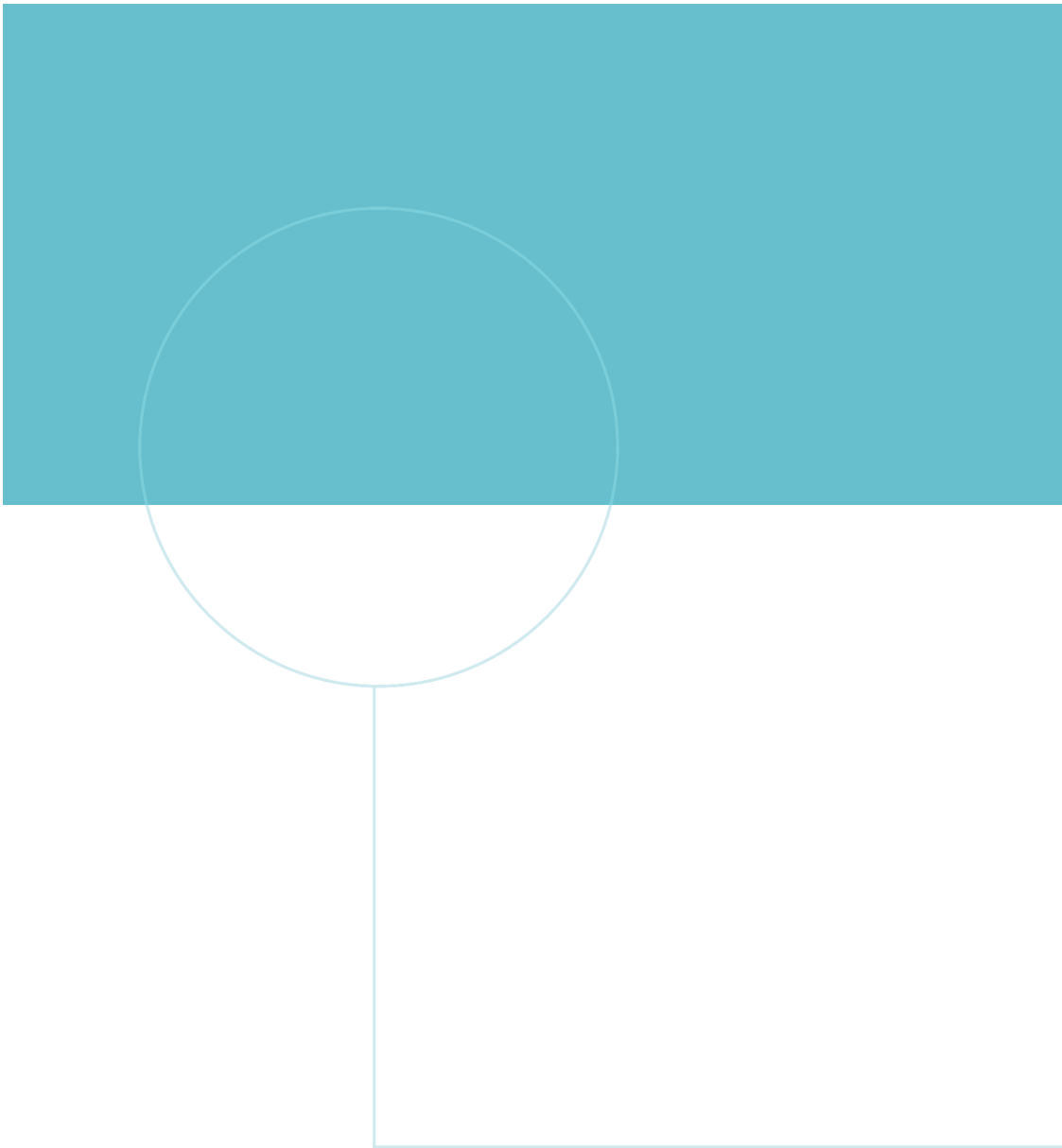

NTNU
Norwegian University of
Science and Technology

UNIVERSITAT DE
BARCELONA